

BLENDING OF LINEAR AND BRANCHED POLYMERS FOR USEFUL MATERIALS

INTERIM REPORT

Period: January 1, 1999 – December 31, 1999

TABLE OF CONTENTS

Summary of Results	3
Scientific Problem and Relevance to Army Needs	4
Literature Review: The Reported Work Placed in Context	5
List of Manuscripts	11
Participating Scientific Personnel	11
Inventions	11
Scientific Progress and Accomplishments	11
I. Synthesis and Characterization of Linear and Branched Polymers	12
II. Bulk Thermodynamic Interactions in Blends of Branched and Linear Polymers	13
III. Surface Segregation in Blends of Branched and Linear Polymers	25
IV. Dynamics: Comparison of Star and Linear Polybutadiene .	44
References	
Technology Transfer	48

REPORT DOCUMENTATION PAGE

Form Approved
OMB NO. 0704-0188

Public reporting burden for this collection of information is estimated to average 1 hour per response, including the time for reviewing instructions, searching existing data sources, gathering and maintaining the data needed, and completing and reviewing the collection of information. Send comment regarding this burden estimate or any other aspect of this collection of information, including suggestions for reducing this burden, to Washington Headquarters Services, Directorate for Information Operations and Reports, 1215 Jefferson Davis Highway, Suite 1204, Arlington, VA 22202-4302, and to the Office of Management and Budget, Paperwork Reduction Project (0704-0188), Washington, DC 20503.

1. AGENCY USE ONLY (Leave blank)		2. REPORT DATE 2/25/00	3. REPORT TYPE AND DATES COVERED Final 05/15/96-2/14/00	
4. TITLE AND SUBTITLE "Blends of Linear and Branched Polymers for Useful Materials"			5. FUNDING NUMBERS DAAH04-96-1-0164	
6. AUTHOR(S) Mark D. Foster, Carmen Greenberg, Teresa Zook				
7. PERFORMING ORGANIZATION NAME(S) AND ADDRESS(ES) The University of Akron The Institute of Polymer Science Akron, OH 44325-3909			8. PERFORMING ORGANIZATION REPORT NUMBER	
9. SPONSORING / MONITORING AGENCY NAME(S) AND ADDRESS(ES) U.S. Army Research Office P.O. Box 12211 Research Triangle Park., NC 27709-2211			10. SPONSORING / MONITORING AGENCY REPORT NUMBER ARO 35053.4-CH	
11. SUPPLEMENTARY NOTES The views, opinions and/or findings contained in this report are those of the author(s) and should not be construed as an official Department of the Army position, policy or decision, unless so designated by other documentation.				
12a. DISTRIBUTION / AVAILABILITY STATEMENT Approved for public release; distribution unlimited.			12 b. DISTRIBUTION CODE	
13. ABSTRACT (Maximum 200 words) The aim is to study the use of molecules of novel architecture for tailoring the surface properties of blends. Key to this work is understanding the bulk miscibility of blends of linear and branched molecules and characterizing the surface segregation that occurs in such blends. The thermodynamic interaction between two polymers due only to the effect of regular branching has been measured for polystyrene blends of linear and star polymers as well as for one blend of a comb polymer with linear chains. Blends of star and linear polybutadiene have been investigated as well. The bulk interaction grows in size with the number of arms in the star. The interaction for the comb/linear blend is an order of magnitude larger than for a star/linear blend in which the star has the same number of arms as the comb. Segregation of the star to both interfaces of a film is observed for the polystyrene blends. For polybutadiene blends the isotopic effect is so strong that for small numbers of arms the isotopic effect dominates. The collective dynamics of two star polybutadienes are seen to be identical to those of linear analogs when the arms have lengths many times the entanglement length.				
14. SUBJECT TERMS Polymer blends, star branched polymers, surface segregation, Interaction parameter, SANS, reflectometry			15. NUMBER OF PAGES	
			16. PRICE CODE	
17. SECURITY CLASSIFICATION OR REPORT UNCLASSIFIED	18. SECURITY CLASSIFICATION OF THIS PAGE UNCLASSIFIED	19. SECURITY CLASSIFICATION OF ABSTRACT UNCLASSIFIED	20. LIMITATION OF ABSTRACT UL	

SUMMARY OF RESULTS

Three aspects of the thermodynamics of blends of linear and long-branched polymers have been studied using well-defined polystyrene and polybutadiene polymers synthesized for this purpose. First, the bulk thermodynamic interactions between the chains of different architecture have been quantified using small angle neutron scattering. Secondly, surface segregation in such blends has been studied using three techniques sensitive to concentration depth profiles near surfaces. Finally, a first step has been taken in studying collective dynamics in such blends by comparing the dynamics of pure melts of linear and star polybutadiene using quasielastic neutron scattering.

The thermodynamic interaction due to architectural differences was quantified for several star/linear blends and one comb/linear blend without making any assertions as to whether this interaction is entropic or enthalpic in origin. However, we find the interaction is strikingly similar in magnitude to the "entropic" contribution predicted by a mean field theory for an athermal blend. Thus the theory's assertion that bulk phase segregation is unlikely for blends of linear chains with stars is substantiated.

The contribution to the interaction parameter ascribable to architectural effects, $\Delta\chi$, increases with star functionality for a series of polystyrene stars, even though theory would suggest that variations in arm size should lead to variations which are not simply monotonic in the number of arms. Agreement with theoretical expectations is seen on two other points, though. First, the variation in χ with composition of the star/linear blend predicted by the theory is seen experimentally, though more compositions should be measured to test this more fully. Second, the interaction between a comb branched chain and its linear analog is much stronger than that between a linear analog and a star with the same number of arms as the comb.

A bulk thermodynamic interaction due to different architecture is also seen in star/linear blends of polybutadiene. The strength of this architectural effect is much larger than that in the PS blends, leading one to anticipate that surface segregation of star branched polymers may be stronger in blends of PB than in blends of PS. However, this is not the case.

In polystyrene star/linear blends the star chains are seen to go preferentially to both interfaces. The strength of the segregation is affected by the labeling, i.e. whether the star or linear chain is deuterated. The labeling effects are unexpected in part, though. Deuterated stars segregate more strongly to a silicon oxide surface, but segregate slightly less strongly to the air surface than do the unlabeled stars. The segregation to the air interface increases slightly with small increases in arm number (4 - 6) for the chains that are similarly linked with silane linking agents. Divinylbenzene (DVB) linked stars with many more arms (12-21) show no greater segregation to the air interface, suggesting that the effect of functionality on degree of segregation is modest. On the other hand the enhancement of segregation to the silicon oxide surface when upon deuteration of the star is much more pronounced for the DVB linked stars.

The picture of the behavior of polybutadiene blends is much less complete, but a few conclusions can be drawn. For small numbers of arms, the stronger isotopic effect for PB dominates the architectural effect, so that, in blends labeled for measurements, the linear species may be preferentially located at the surface. It is nonetheless expected that in the absence of labeling the star will go to both the surface and substrate interface, but not so strongly as in the case of polystyrene. The strength of the segregation is not much changed by a nearly four-fold change in the molecular weight of the linear component.

Quasielastic neutron scattering measurements were made from samples of pure linear polybutadiene and pure four arm and six arm star polybutadiene at three widely spaced temperatures above and below the glass transition temperature. The scattering changes with temperature in an

expected way, with the broad Boson peak visible at low temperatures. No differences between the dynamics of the linear and star branched chains are seen for either the four-arm or six-arm stars. This is true both above and below the glass transition temperature. For arms of lengths several times the entanglement molecular weight the tethering to the core plays no role in the low energy collective dynamics.

SCIENTIFIC PROBLEM AND RELEVANCE TO ARMY NEEDS

The blending of polymers is a proven means of tailoring the bulk properties of materials to specific applications. The tailored synthesis of novel molecules for targeted blending of materials to simultaneously provide tailored surface properties and bulk properties is the motivation for the research described here. In particular, this research investigates the fundamental phenomena that control the bulk miscibility and surface enrichment in blends of linear and long-branched polymers. The development of synthesesⁱ for a variety of branched molecular architectures including regular stars and combs has made it possible to consider intentional blending of linear molecules with a minority component having a nonlinear architecture designed to provide tailored processing properties and/or tailored surface properties through controlled surface segregation.

There is already considerable appreciationⁱⁱ for the fact that star-branched and comb polymers have properties differing from those of their linear counterparts. In particular, solutions of branched molecules have lower viscosities and therefore star materials are used as shear stable viscosity modifiersⁱⁱⁱ. Melts containing branched polymers also have interesting rheological properties and Exxon markets blends of star-branched and linear butyl elastomers which reportedly^{iv} have mechanical properties comparable to conventional linear materials, but better processing characteristics.

To illustrate the motivation for tailoring surface properties through branched/linear blends one may consider the hypothetical case of an elastomeric material which is required to have both good chemical resistance and good dynamic properties. Existing elastomers which provide optimal performance with respect to chemical resistance may provide poor dynamical properties. An example is Neoprene, which has much better chemical resistance than natural rubber or synthetic polyisoprene, but which has worse dynamic properties. Since chemical resistance is needed first and foremost at the surface, an elastomeric material which has an enriched chlorine content in the surface region, but predominantly unchlorinated molecules in the bulk could combine the desired surface chemical resistance and favorable bulk dynamic properties. In general, however, attempts to mix dissimilar elastomers lead to macroscopic phase segregation, which is undesirable.

A solution to this problem is a miscible two component system in which the chemically resistant species is a small minority, but this minority component goes to the surface preferentially. In the case of a chlorinated versus unchlorinated elastomer the chlorinated molecule would typically be driven *away* from the surface due to its higher surface energy. On the other hand, this effect can be counterbalanced using competing architectural effects which favor more highly branched molecules at an interface, all other things being equal. Thus, a lightly chlorinated elastomer molecule could be driven to segregate to the surface using architectural effects.

A second example application would be the design of a new elastomer for gas masks in which impermeability to chemical agents is a key bulk property, but a small region of silicon based rubber surface next to the skin can provide better comfort. Since the silicon rubber has lower surface energy it is favored at the surface, but the challenge is to create a polymer which saturates that surface with siloxane segments while ensuring that the surface layer is not mechanically separated from the bulk material.

In this work, the tendency to bulk demixing and surface enrichment due to long-chain branching is quantified. Also, the potential for creating polymeric blends with tailored property gradients near the surface using branched molecules is probed. This research complements that being done within the Army and by other Army contractors on materials containing very highly branched polymers known as "dendrimers" or "hyperbranched polymers".

- i. S. Bywater, "Preparation and Properties of Star-branched Polymers," *Adv. Polym. Sci.* **1979**, *30*, 89.
- ii. Grest, G. S.; Fetters, L.J.; Huang, J.S.; Richter, D. "Star Polymers: Experiment, Theory, and Simulation," *Adv. Chem. Phys.* **1996**, *94*, 67.
- iii. Mishra, M.K.; Saxton, R.G. "Polymer additives for engine oils," *Chemtech* **1995**, *25*, 35. Eckert, R. J. A. "Hydrogenated Star-Shaped Polymer," U.S. Patent 4 116 917, 1978.
- iv. Soskey, P.R.; Duvdevani, I.; Wang, H.C.; Richards, T.E. "Star Branched Butyl: A Novel Butyl Rubber for Improved Processability. III. Polymer Rheology," *Proceedings of Rubber Division, American Chemical Society*, Detroit, Michigan, October 17-20, **1989**.

LITERATURE REVIEW: THE REPORTED WORK PLACED IN CONTEXT

Bulk Behavior

The bulk thermodynamic behavior of binary polymer blends has been found to be sensitive to a number of subtle differences between the components including chemical microstructure¹⁻³, tacticity⁴, and the degree and type of isotopic labeling⁵. Small Angle Neutron Scattering measurements have played an important role in studies of these effects and therefore isotopically labeled blends have been the focus of study. Differences in branching between the two components can also lead to thermodynamic interactions in the bulk⁶ and this effect is the focus of the work presented here. Comparatively recent theoretical work has been done for blends containing regular stars^{7,8} or regular combs^{6,8} and for blends of linear and randomly branched homopolymers⁹⁻¹¹.

Only a few experimental studies¹²⁻¹⁸ have been done on the thermodynamics of blends of branched and linear chains. One grouping of these studies comprises those dealing with short chain branching^{12,13} while another has considered blends with long chain branched components¹⁴⁻¹⁸. Both Faust *et al.*¹⁴ and Russell *et al.*¹⁵ considered the change in the behavior of miscible blends of polystyrene (PS) and poly(vinyl methyl ether) (PVME) when the architecture of the PS was changed from linear to star-shaped. Faust *et al.*¹⁴ argued that when changing from a linear PS to a 22 arm star the temperature of the minimum in the cloud point curve did not shift (once corrections for sluggish kinetics were considered), but the shape of the cloud-point curve changed subtly. Russell *et al.*¹⁵ found that the minimum in the cloud point curve moved up by about 10°C when linear PS in a PS/PVME blend was replaced by a well-defined four-arm PS star. Furthermore, replacing the PS star with a deuterated star led to an additional increase of about 10 °C. The primary focus of the work by Russell *et al.*¹⁵ was consideration of the impact of changing architecture on concentration fluctuations in PS/PVME blends. However, Russell and coworkers report having measured the SANS blends of normal star and deuterated star PS for a range of compositions, showing a single scattering curve for the 50/50 blend. Their objective was to clarify the appropriate single chain scattering function for the star polymers. The scattering was not reported in absolute units and no value of χ for the star/star blend was reported.

Initial experimental results from this group for the interaction found in blends of four-arm stars and linear polystyrene analogs have been published¹⁸. There we noted that the magnitude of

the interaction, while small, was measurable and was close in magnitude to that anticipated by the theory of Fredrickson *et al.*⁶

Fredrickson and coworkers⁶ considered athermal binary blends in which the components are identical in chemistry, but of various architectures, *i.e.* star-branched or comb-branched homopolymers mixed with linear chains as compared to linear/linear homopolymer blends. The conventional interaction parameter, χ , is expressed in terms of an invariant α , which is independent of how the statistical segments of the blend components are defined^{19,20},

$$\chi = \alpha(v_1 v_2)^{1/2}, \quad (1)$$

where v_1 and v_2 represent the volumes of the statistical segments of the blend components. These authors assume that α may be thought to contain two contributions, an enthalpic contribution $A(\phi)$ and an entropic contribution $B(\phi)$, with

$$\alpha = A(\phi)/T + B(\phi). \quad (2)$$

For blends of star/linear homopolymers the entropic contribution to α , referred to as α_e , may be expressed in terms of the number of arms, p , and the arm radius of gyration, R_2 (radius of gyration $R_2^2 = N_2 b^2 / 6$), where N_2 is the number of segments in one arm, and b is the segment length. For stars with a large number of short arms or for large homopolymers for which the condition $(p-3)(R_1/R_2)^2 \gg 1$ is met, where R_1 is the radius of gyration of the linear chain, the universal form of α_e is given by

$$\alpha_e \sim \frac{1}{64\pi\sqrt{2}} \frac{(p-3)^{3/2}}{(1-\phi_1)^{1/2} R_2^3}, \quad (3)$$

where ϕ_1 is the volume fraction of the linear component in the binary blend. Fredrickson and coworkers⁶ concluded that χ should be small in the case of star branched polymers with linear analogs, with the size of the effective interaction increasing with increasing number of arms and increasing disparity between the size of the linear chains and the size of the star arms. The effect for bulk miscibility is subtle and bulk phase segregation is predicted to be unlikely for modest numbers of arms of polymeric length.

For the case of comb/linear homopolymer binary blends⁶, the restriction that only large numbers of arms be considered is removed from the theory. The authors considered combs with regularly spaced branches of M statistical segments, spaced along the backbone every L statistical segments. The value of α_e may be much larger because there are more branched points per molecule than in the case of the star homopolymers. Bulk phase separation is favored for combs with closely spaced short branches. For overall molecular volumes of the linear and comb polymers that are comparable and for L comparable to M , phase segregation is predicted to occur when M is of the order of $N_1^{2/3}$, where N_1 is the number of segments in the linear chain. Fredrickson *et al.*⁶ concluded that for linear/comb homopolymer blends phase separation should be easily accomplished in practice. Experimental studies on blends of linear and *short* branched polyethylenes^{12,13} have shown that for low branch content (< 4 branches/100 backbone carbon atoms for $M_w \sim 10^5$) the mixtures are

homogenous while for higher numbers of branches (> 8 branches/100 backbone carbon atoms) the blends are found to phase separate.

For model polyolefins, theoretical as well as experimental studies^{5,21-24} suggest that the interactions between saturated hydrocarbons of differing molecular architecture may often be satisfactorily rationalized considering simple enthalpic arguments. For isotopic blends of saturated hydrocarbons, χ has been found to increase when the polymer with more short chain branching is deuterated⁵. These findings are consistent with a simple theory expressing χ in terms of the solubility parameters of a blend's components. Deuteration reduces the solubility parameter of a component slightly⁵. Changes in molecular architecture leading to changes in contact density also alter solubility parameters. Further support for this view is provided by simulations performed by Maranas *et al.*^{23,24}. These authors suggest a link between the thermodynamic interactions, which are found to be primarily enthalpic in nature, and differences in local packing. A correlation among regular mixing, thermodynamic interaction parameter, χ , and solubility parameters is found.

In the study at hand the thermodynamic interactions between regular, long branched chains and linear analogs are quantified for a series of blends using small angle neutron scattering. The primary objective is to provide experimental results on well-defined blends that can serve as a basis for comparison in the development of theoretical treatments. Key to the study are the preparation of the requisite polymers of well-defined architecture and molecular weight and the use of isotopic blends. While the primary focus is on the change in interaction with number of arms and type of branching (star vs. comb), changes in χ with labeling scheme and blend composition are addressed as well.

Surface Segregation

The segregation of one species preferentially to the surface of a binary polymer blend has been studied recently both theoretically²⁵⁻³⁷ and experimental³⁸⁻⁴⁸. Theoretical and experimental studies on isotopic blends of linear polystyrene (PS) have shown that surface segregation of one component can be driven by molecular weight differences^{25-27,44,45,49}, differences in chain-end functionalization^{25,26,34,50,51}, and even deuteration^{28,39,44,45,52}. For isotopic blends of PS of symmetric molecular weights, the deuterated species segregates to surfaces and interfaces due to the differences in bond length and bond polarizability between the C-H and the C-D bonds. The surface energy of the deuterated PS is slightly lower.

In addition to these effects which have already been experimentally demonstrated, differences in chain architecture have been predicted to be another effect which can lead to surface segregation³⁶. The more highly branched polymer chain has been predicted to segregate to the surface. In particular, in a mixture of linear and star branched polymers which are otherwise identical, theoretical studies have predicted that the star chains should be preferred at the surface³⁶. Three reasons for this predicted behavior have been suggested. First, star components are characterized by a higher number of chain ends than are linear polymers of the same molecular weight^{26,34,40,53} and these ends are preferred at the surface. A second possible cause of star segregation to the surface could be the lower segment contact density of the stars. The number of contacts per chain is reduced for chains that are moved from the bulk to a surface. Since the contact density for stars is lower, the system minimizes the loss of favorable enthalpic interaction by putting stars at the surface. Finally, a third possible cause is the reduced conformational entropy for star chains as compared to their linear analogs. Chains suffer a loss in possible number of configurations

when moving from the bulk to the surface. Moving stars to surfaces and interfaces is therefore entropically preferred.

The extent to which surface segregation is driven by entropic and enthalpic contributions was studied theoretically by Yethiraj³³. Using Monte Carlo simulations he examined a blend of short, branched and linear polymers of the same molecular weight. For an athermal system, *i.e.*, a system containing no enthalpic interactions, Yethiraj predicted a depletion of the branched component from the surface. The surface excess of linear chains is very small, and according to the author, probably not measurable in experiments. When energetic attractions within and between chains are introduced into the simulations, the branched component is predicted to segregate to the surface. This is due to the fact that in this case the linear chains pack more efficiently than do the branched polymer chains. Thus the system's overall free energy is minimized by locating the linear chains in the bulk where the coordination number is higher. Yethiraj's study therefore suggests that the surface segregation in a branched/linear blend is driven by enthalpic considerations.

Wu and Fredrickson³⁶ examined the surface segregation in binary blends of architecturally asymmetric components of the same type of monomer using a mean-field description of chain statistics and using a self-consistent field theory in the spirit of Edwards and Helfand. Specific examples of regular star/linear, regular comb/linear, and ring/linear blends were considered. Their findings suggest that branching produces surface-active ends and junctions, where the ends are attracted to the surface while the junctions are repelled from the surface by entropic forces. They consider this behavior universal and independent of the chemical nature of the two components in the blend in the case in which the branches are sufficiently long and the junctions are dilute. For dilute mixtures of stars added to a matrix of linear chains the authors have calculated the dependence of surface enrichment on the number of arms, p , the length of the arms, L , and the strength of the enthalpic contribution to the surface potential for ends. They found that as the number of arms is increased, the net entropic attraction for ends (scaling as p) dominates over the repulsion of the junction [scaling as $\log(p)$], and the amount of star segregated to the surface increases. An increase in star surface segregation was also seen when the length of the arms is decreased, and when the chain ends of the stars are given attractive interactions with the surface.

Recent experimental work has been done by Mayes and coworkers⁵⁴ on surface segregation in blends of linear homopolymer and comb branched copolymer. The intent was to use differences in chain architecture as a basis for entropically driving enthalpically unfavorable chain segments to the surface. The authors studied randomly branched copolymers with poly(methyl methacrylate) (PMMA) backbones and methoxy poly(ethylene glycol) monomethacrylate (P(MMA-r-MnG)) branches. The branches were terminated with methyl units. They showed that in blends of PMMA with P(MMA-r-MnG) the branched component is found at the air surface as well as at the substrate interface, even though the branched component is thought to be characterized by a higher surface energy.

In the work described below, the interfacial segregation in blends of linear and well-defined regularly branched polystyrenes and polybutadienes is explored. The extent of segregation at both the air and substrate interfaces are quantified using neutron reflectometry (NR), dynamic secondary ion mass spectroscopy (DSIMS), and nuclear reaction analysis (NRA).

References for Literature Review

- (1) Sakurai, S.; Hasegawa, H.; Hashimoto, T.; Glen Hargis, I.; Aggarwal, S. L.; Han, C. C. *Macromolecules* **1990**, *23*, 451.

- (2) Sakurai, S.; Jinnai, H.; Hasegawa, H.; Hashimoto, T.; Han, C. C. *Macromolecules* **1991**, *24*, 4839.
- (3) Rhee, J.; Crist, B. *Macromolecules* **1991**, *24*, 5663.
- (4) Beaucage, G.; Stein, R. S.; Hashimoto, T.; Hasegawa, H. *Macromolecules* **1991**, *24*, 3443.
- (5) Graessley, W. W.; Krishnamoorti, R.; Balsara, N. P.; Fetters, L. J.; Lohse, D. J.; Schultz, D. N.; Sissano, J. A. *Macromolecules* **1993**, *26*, 1137.
- (6) Fredrickson, G. H.; Liu, A.; Bates, F. S. *Macromolecules* **1994**, *27*, 2503.
- (7) Garas, G.; Kosmas, M. *Macromolecules* **1994**, *27*, 6671.
- (8) Gujrati, P. D. *J. Chem. Phys.* **1998**, *108*, 5104.
- (9) Roby, F.; Joanny, J.-F. *Macromolecules* **1991**, *24*, 2060.
- (10) Gujrati, P. D. *J. Chem. Phys.* **1998**, *108*, 5089.
- (11) Clarke, N.; McLeish, T. C. B.; Jenkins, S. D. *Macromolecules* **1995**, *28*, 4650.
- (12) Alamo, R. G.; Londono, J. D.; Mandelkern, L.; Stehling, F. C.; Wignall, G. D. *Macromolecules* **1994**, *27*, 411.
- (13) Alamo, R. G.; Graessley, W. W.; Krishnamoorti, R.; Lohse, D. J.; Londono, J. D.; Mandelkern, L.; Stehling, F. C.; Wignall, G. D. *Macromolecules* **1997**, *30*, 561.
- (14) Faust, A. B.; Sremcieh, P. S.; Gilmer, J. W.; Mays, J. W. *Macromolecules* **1989**, *22*, 1250.
- (15) Russell, T. P.; Fetters, L. J.; Clark, J. C.; Bauer, B. J.; Han, C. C. *Macromolecules* **1990**, *23*, 654.
- (16) Tsukahara, Y.; Inoue, J.; Ohta, Y.; Kohjiya, S. *Polymer* **1994**, *35*, 5785.
- (17) van Aert, H. A. M.; van Genderen, M. H. P.; Meijer, E. W. *Polym. Bull.* **1996**, *37*, 273.
- (18) Greenberg, C. C.; Foster, M. D.; Turner, C. M.; Corona-Galvan, S.; Cloutet, E.; Butler, P. D.; Hammouda, B.; Quirk, R. P. *Polymer* **1999**, *40*, 4713.
- (19) Helfand, E.; Sapse, A. M. *J. Chem. Phys.* **1975**, *62*, 1327.
- (20) Roe, R. J.; Zin, W. C. *Macromolecules* **1980**, *13*, 1221.
- (21) Graessley, W. W.; Krishnamoorti, R.; Reichart, G. C.; Balsara, N. P.; Fetters, L. J.; Lohse, D. J. *Macromolecules* **1995**, *28*, 1260.
- (22) Balsara, N.; Fetters, L. J.; Hadjichristidis, N.; Lohse, D. J.; Han, C. C.; Graessley, W. W.; Krishnamoorti, R. *Macromolecules* **1992**, *25*, 6137.
- (23) Maranas, J. K.; Mondello, M.; Grest, G. S.; Kumar, S. K.; Debenedetti, P. G.; Graessley, W. W. *Macromolecules* **1998**, *31*, 6991.
- (24) Maranas, J. K.; Mondello, M.; Grest, G. S.; Kumar, S. K.; Debenedetti, P. G.; Graessley, W. W. *Macromolecules* **1998**, *31*, 6998.
- (25) Hariharan, A.; Kumar, S. K.; Russell, T. P. *Macromolecules* **1990**, *23*, 3584.
- (26) Hariharan, A.; Kumar, S. K.; Russell, T. P. *Macromolecules* **1991**, *24*, 4909.
- (27) Hariharan, A.; Kumar, S. K.; Russell, T. P. *J. Chem. Phys.* **1993**, *98*, 4163.
- (28) Hariharan, A.; Kumar, S. K.; Russell, T. P. *J. Chem. Phys.* **1993**, *98*, 6516.
- (29) Hariharan, A.; Kumar, S. K.; Rafailovich, M. H.; Sokolov, J.; Zheng, X.; Duong, D.; Schwarz, S. A.; Russell, T. P. *J. Chem. Phys.* **1993**, *99*, 656.
- (30) Fredrickson, G. H.; Donley, J. P. *J. Chem. Phys.* **1992**, *97*, 8941.
- (31) Yethiraj, A.; Kumar, S. K.; Hariharan, A.; Schweizer, K. S. *J. Chem. Phys.* **1994**, *100*, 4691.
- (32) Yethiraj, A. *J. Chem. Phys.* **1994**, *101*, 2489.
- (33) Yethiraj, A. *Phys. Rev. Lett.* **1995**, *74*, 2018.
- (34) Wu, D. T.; Fredrickson, G. H.; Carton, J.-P.; Ajdari, A.; Leibler, L. *J. Polym. Sci. B: Polym. Phys.* **1995**, *33*, 2372.
- (35) Wu, D. T.; Fredrickson, G. H.; Carton, J.-P. *J. Chem. Phys.* **1996**, *104*, 6387.
- (36) Wu, D. T.; Fredrickson, G. H. *Macromolecules* **1996**, *29*, 7919.
- (37) Walton, D. G.; Mayes, A. M. *Phys. Rev. E.* **1996**, *54*, 2811.

- (38) Jones, R. A. L.; Kramer, E. J.; Rafailovich, M. H.; Sokolov, S.; Schwarz, S. A. *Mat. Res. Soc. Symp. Proc.* **1989**, *153*, 133.
- (39) Jones, R. A. L.; Norton, L. J.; Kramer, E. J.; Composto, R. J.; Stein, R. S.; Russell, T. P.; Mansour, A.; Karim, A.; Feltcher, G. P.; Rafailovich, M. H.; Sokolov, J.; Zhao, X.; Schwarz, S. A. *Europhys. Lett.* **1990**, *12*, 41.
- (40) Zhao, W.; Zhao, X.; Rafailovich, M. H.; Sokolov, J.; Composto, R. J.; Smith, S. D.; Sarkowski, M.; Russell, T. P.; Dozier, W. D.; Mansfield, T. *Macromolecules* **1993**, *26*, 561.
- (41) Zhao, X.; Zhao, W.; Sokolov, J.; Rafailovich, M. H.; Schwartz, S. A.; Wilkens, B. J.; Jones, R. A. L.; Kramer, E. J. *Macromolecules* **1991**, *24*, 5991.
- (42) Sokolov, J.; Rafailovich, M. H.; Jones, R. A. L.; Kramer, E. J. *Appl. Phys. Lett.* **1989**, *54*, 590.
- (43) Hong, P. P.; Boerio, F. J.; Clarson, S. J.; Smith, S. D. *Macromolecules* **1991**, *24*, 4770.
- (44) Hong, P. P.; Boerio, F. J.; Smith, S. D. *Macromolecules* **1993**, *26*, 1460.
- (45) Hong, P. P.; Boerio, F. J.; Smith, S. D. *Macromolecules* **1994**, *27*, 596.
- (46) Fleischer, C. A.; Koberstein, J. T.; Krukoni, V.; Wetmore, P. A. *Macromolecules* **1993**, *26*.
- (47) Elman, J. F.; Hons, B. D.; Long, T. E.; Koberstein, J. T. *Macromolecules* **1994**, *27*, 5341.
- (48) Schaub, T. F.; Kellogg, G. H.; Mayes, A. M.; Kulasekera, R.; Ankner, J. F.; Kaiser, H. *Macromolecules* **1996**, *29*, 3982.
- (49) Kumar, S. K.; Russell, T. P. *Macromolecules* **1991**, *24*, 3584.
- (50) Affrossman, S.; Bertrand, P.; Hartshorne, M.; Kiff, T.; Leonard, D.; Pethrick, R. A.; Richards, R. W. *Macromolecules* **1996**, *29*, 5432.
- (51) Jalbert, C.; Koberstein, J. T.; Hariharan, A.; Kumar, S. K. *Macromolecules* **1997**, *30*, 4481.
- (52) Jones, R. A. L.; Kramer, E. J.; Rafailovich, M. H.; Sokolov, J.; Schwarz, S. A. *Phys. Rev. Lett.* **1989**, *62*, 280.
- (53) Affrossman, S.; Hartshorne, M.; Jerome, R.; Pethrick, R. A.; Petitjean, S.; Vilar, M. R. *Macromolecules* **1996**, *26*, 6251.
- (54) Walton, D. G.; Soo, P. P.; Mayes, A. M.; Allgor, S. J. S.; Fujii, J. T.; Griffith, L. G.; Ankner, J. F.; Kaiser, H.; Johansson, J.; Smith, G. D.; Barker, J. G.; Satija, S. K. *Macromolecules* **1997**, *30*, 6947.

LIST OF MANUSCRIPTS

1. Greenberg, C. C.; Foster, M. D.; Turner, C. M.; Corona-Galvan, S.; Cloutet, E.; Butler, D. P.; Hammouda, B.; Quirk, R. P. "Effective Interaction Parameter Between Topologically Distinct Polymers", *Polymer* 40 (16), 4713-4716, 1999.
2. Greenberg, C. C.; Foster, M.D.; Teale, D. M.; Turner, C. M.; Cloutet, E.; Corona-Galvan, S.; Quirk, R. P.; Butler, P.; Majkrzak, C.F. "Thermodynamics of Blends of Linear and Branched Polymers: Bulk and Surface Behavior," *Bull. Amer. Phys. Soc.* 1999, 44(1), Part II, 1909.
3. M.D. Foster, C.C. Greenberg, D.M. Teale, C.M. Turner, S. Corona-Galvan, E. Cloutet, P.D. Butler, B. Hammouda, R.P. Quirk, "Effective χ and Surface Segregation in Blends of Star and Linear Polystyrene," *Makromolekulare Chemie - Macromolecular Symposia*, submitted 6/8/99.
4. C. C. Greenberg, M. D. Foster, C. M. Turner, S. Corona-Galvan, E. Cloutet, R. P. Quirk, P.D. Butler, B. Hammouda, C. Hawker, "Effective Interaction Parameter Between Branched and Linear Polystyrene", in preparation.
5. C. C. Greenberg, D. M. Teale, M. D. Foster, C. M. Turner, S. Corona-Galvan, E. Cloutet, R. P. Quirk, C. F. Majkrzak, D. Demaree, "Surface Segregation in Blends of Linear and Regularly Star Branched Polystyrene," in preparation.

PARTICIPATING SCIENTIFIC PERSONNEL

Dr. Mark D. Foster, Professor

Dr. Roderick P. Quirk, Professor

Carmen C. Greenberg, Ph.D. Univ. Akron awarded 12/99

Teresa Martter, Ph.D. candidate - Lord Corporation Fellowship awardee

INVENTIONS

None

SCIENTIFIC PROGRESS AND ACCOMPLISHMENTS

In summary, work this year extended the number of molecules studied by considering stars of higher functionality and by moving ahead substantially in the measurement of surface segregation effects. In particular, a collaboration with ARL on depth profiling with nuclear reaction analysis, initiated in '98, resulted in data for several samples. One paper was submitted to *Makromolekulare Chemie - Macromolecular Symposia*, a thesis was completed and two additional papers from that thesis nearly completed before illness of a key author delayed completion. These two papers are in nearly final form and it is anticipated that they will be submitted to *Macromolecules* in the next 60 days. The PI gave two invited talks in Europe and has been invited to present the work at an international meeting in Germany in September 2000.

The following description of the progress has been broken into three sections. The first describes briefly the molecules made for the study. A second section discusses the study of bulk thermodynamic effects. In the third section the surface segregation of both polystyrene blends and polybutadiene blends is described. In the fourth and final section the dynamics of star chains are compared with those of linear chains.

I. SYNTHESIS AND CHARACTERIZATION OF LINEAR AND BRANCHED POLYMERS

The characteristics of all the star and linear polystyrene polymers used in the work are given in Table 1. Those made in this year are marked with an asterisk. The comb polymer is also mentioned for the first time this year. A six branch comb PS was synthesized by Craig Hawker at the IBM Laboratories¹. While the linear and star polymers were synthesized using anionic polymerization, the comb was synthesized using living free radical polymerization. The comb polymer had a larger polydispersity index than did the star polymers and the number of arms per

Table 1. Molecular Characterization of Star and Linear Polystyrenes

Polymer	Sample	Arms	M_n (g/mol)	R_g^a (Å)	N^b		PI
Linear hPS & dPS							
Hydrogenous PS	hPS	-	50,000	60	484		1.03
Hydrogenous PS	hPS	-	132,000	97	1,27		1.03
Hydrogenous PS	hPS	-	212,000	123	2,040		1.04
Hydrogenous PS	hPS	-	231,000	129	2,220		1.04
Deuterated PS	dPS	-	143,000	98	1,280		1.05
Deuterated PS	dPS	-	252,000	130	2,250		1.08
Deuterated PS	dPS	-	391,000	161	3,490		1.05
Deuterated PS	dPS	-	674,000	212	6,010		1.08
Silane-Linked PS Stars							
Deuterated 4-arm star	d4s	4	100,000	65	893	223/arm	1.02
Hydrogenous 4-arm star	h4s	4	85,000	62	817	204/arm	1.02
Deuterated 5-arm star	d5s	5	164,000	76	1,460	293/arm	1.11
Hydrogenous 5-arm star	h5s	5	131,000	70	1,260	252/arm	1.19
Deuterated 6-arm star	d6s	6	157,000	68	1,410	234/arm	1.10
Hydrogenous 6-arm star	h6s	6	192,000	75	1,710	286/arm	1.17
Hydrogenous 8-arm star	h8s	8	390,000	98	3,750	469/arm	1.07
DVB-Linked PS Stars							
Hydrogenous 12-arm *	hDVB12	12	140,000	49	1,350	112/arm	1.04
Hydrogenous 14-arm *	hDVB14	14	290,000	65	2,790	200/arm	1.09
Hydrogenous 17-arm *	hDVB17	17	190,000	48	1,830	107/arm	1.06
Hydrogenous 21-arm *	hDVB21	21	650,000	81	6,250	289/arm	1.17
Deuterated 15-arm *	dDVB15	15	200,000	50	1,790	119/arm	1.04
Deuterated 16-arm *	dDVB16	16	200,000	49	1,790	112/arm	1.05
Comb PS Polymer							
Hydrogenous 6-branch *	h6c	6	69,000	46	663	63/arm	1.35

^a. Calculated using well established formula for the linear chains and estimated for the stars

^b. Assuming a segment volume of 100 cm³/mol.

molecule varied more than for the stars. The branches were attached to the backbone with a benzyl group ($C_6H_5-O-CH_2$ polystyrene arms), which allowed for the branches to be cleaved off in order to check their molecular weight and polydispersity. An alkoxyamine functionality was present at the outer end of each branch.

The chain lengths in terms of the numbers of segments in a chain, N , are given for a segment volume of $100 \text{ cm}^3/\text{mol}$. For the stars N_{arm} is given as well. Radii of gyration (R_g) for the linear chains were calculated using $R_g^2 = \frac{a^2 N}{6}$, where a is the length of the statistical segment taken as $a = 6.7 \text{ \AA}^2$ for both the star and the linear chains. Radii of gyration for the stars were estimated by correcting the calculated R_g for the corresponding linear chain by the g factor for the appropriate number of arms using the theory of Zimm and Stockmayer³.

The polybutadiene materials synthesized anionically are described in Table 2. Again, those materials new to this year's report are marked with an asterisk. The linear materials were purchased and the stars synthesized in Prof. Quirk's laboratory.

Table 2. Molecular Characteristics of Polybutadiene Materials

Polybutadiene	Sample	M_n (g/mol)	N^a	M_w/M_n	% 1,4 addition	Linking agent
Linear	hPB	88,000	1627	1.07	>90	-
High MW Linear*	hPB2	364,000	6066	1.12	82	-
Deuterated Linear*	dPB	92,000	1531	1.04	82	-
4-arm Star	h4sPB	95,000	1756	1.05	>90	$SiCl_4$
6-arm Star *	h6sPB	121,000	2214	1.01	>90	$Cl_3Si-(CH_2)_6-SiCl_3$
8-arm Star *	h8sPB	114,000	2114	1.06	>90	$Si-(CH_2CH_2-SiCl_2-CH_3)_4$

^aAssuming a segment volume of $60.22 \text{ cm}^3/\text{mole}$.

II. BULK THERMODYNAMIC INTERACTIONS IN BLENDS OF BRANCHED AND LINEAR POLYMERS

Measuring the thermodynamic interactions between star and linear chains in the bulk is important both for understanding the surface behavior as well as for understanding the processing behavior and bulk properties of materials made with blends of branched and linear chains. In last year's interim report we presented first results for polystyrene blends containing four arm stars and polybutadiene blends containing four arm stars. This year we have results for a wide range of polystyrene functionalities. After describing the sample preparation and scattering experiments we then describe briefly the analysis of the data and present the results.

Polystyrene

Sample Preparation. Polystyrene blends containing 18 wt% star (either hydrogenous or deuterated) with 82 wt % of the contrasting linear analog were prepared by dissolving the polymers in toluene. One sample blend of composition 50 wt % was also prepared. The solutions were filtered three times using $0.45 \mu\text{m}$ pore size nylon filters and then cast into films in Teflon® beakers, allowing seven days in a fume hood for evaporation of the solvent. The films were then dried under roughing vacuum (10^{-3} Torr) at $70 \text{ }^\circ\text{C}$ for seven days to ensure removal of excess toluene. The dried

polymer blend films were pressed inside brass rings of thickness 1 mm. To obtain transparent, bubble free films, the samples were pressed at 120 °C under 2500 lbs_f between pieces of Mylar® foil. A summary of the samples investigated and the nomenclature used is shown in Table 2.

Table 2. Blend Nomenclature, Compositions, and Sizes of Components

Sample	Component 1	% wt of 1	N_1^a	Component 2	N_2^b
dPS100k	dPS143k	18	1,280	hPS132k	1,270
hPS100k	hPS123k	18	1,270	dPS143k	1,280
d4s100k	d4s	18	893	hPS132k	1,270
h4s100k	h4s	18	817	dPS143k	1,280
h5s200k	h5s	18	1,260	dPS252k	2,250
d5s200k	d5s	18	1,460	hPS231k	2,220
50d6s200k	d6s	50	1,410	hPS231k	2,220
d6s200k	d6s	18	1,410	hPS231k	2,220
h6s200k	h6s	18	1,710	dPS252k	2,250
h6s100k	h6s	18	1,710	dPS143k	1,280
h8s400k	h8s	18	3,750	dPS391k	3,490
hDVB12	hDVB12	18	1,350	dPS143k	1,280
hDVB14	hDVB14	18	2,790	dPS252k	2,250
hDVB17	hDVB17	18	1,830	dPS252k	2,250
hDVB21	hDVB21	18	6,250	dPS674k	6,010
dDVB15	dDVB15	18	1,790	hPS212k	2,040
dDVB16	dDVB16	18	1,790	hPS212k	2,040
h6c	h6c	18	663	dPS50k	484

^a Chain length of component 1.

^b Chain length of component 2.

Scattering measurements. Small angle neutron scattering measurements were performed on the NG3 30-m SANS instrument at the Cold Neutron Research Facility of the National Institute for Standards and Technology in Gaithersburg, Maryland. A neutron beam of wavelength, λ , of 6 Å with a resolution of $\Delta\lambda/\lambda$ of about 0.150 FWHM was used. The chosen instrumental set-up chosen used a sample to detector distance of 13 m which provided a range of scattering vector q ($= 4\pi\sin\theta/\lambda$) of 0.005 – 0.05 Å⁻¹ with a resolution⁴ of approximately 0.005 Å⁻¹.

The samples, sandwiched between quartz windows, were placed in sample holders provided by the NIST laboratory. The sample holders were then placed inside a seven slot computer controlled aluminum sample changer, the temperature of which could be controlled between room temperature and 225 °C (± 0.5 °C). This sample changer sat inside a stainless steel vacuum chamber which was evacuated to a dynamic vacuum of about 10^{-2} Torr. Equilibration times of *ca.* 15 min were allowed after each setpoint change to ensure thermal equilibrium.

In addition to measurements of the samples, other measurements were performed in order to be able to reduce and normalize the data. These included measurements of the empty cell (quartz windows only), the blocked beam and empty beam (for background estimation), standard samples, sample transmission, and standard and empty cell transmissions. All measurements were performed under the same conditions and with the same instrument configuration.

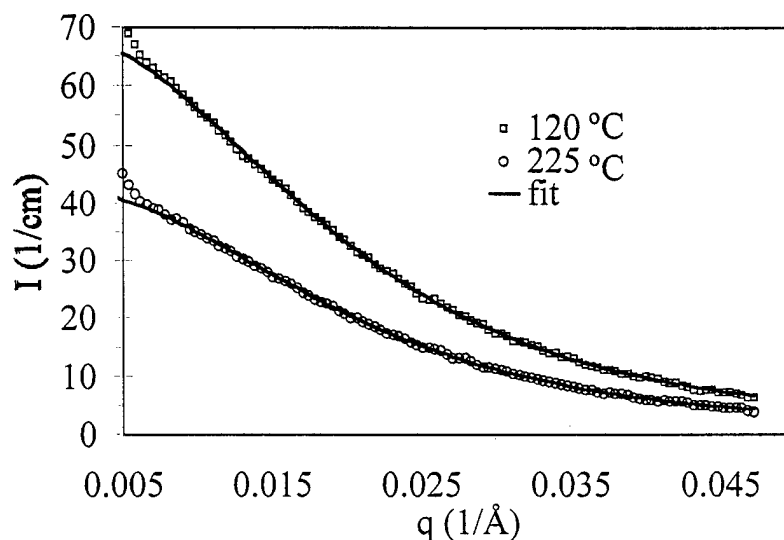


Figure 1. SANS experimental data with fits to the RPA (-) for a blend of 18 wt % deuterated 6-arm star in a matrix of hydrogenous linear PS of symmetric molecular weight (sample d6s200k) for two temperatures: 120 °C (squares) and 225 °C (circles).

Examples of scattering curves obtained for an 18 wt% star/linear blend at 120 °C and 225 °C are given in Figure 1. The absolute coherent scattering intensity, $I(q)$, obtained from a single phase binary isotopic polymer mixture is related to the structure factor $S(q)$ by

$$[I(q)]_{\text{measured}} = \frac{(b_1 - b_2)^2}{(V_1 V_2)^{1/2}} S(q), \quad (4)$$

where b_i and V_i are the segment scattering length and segment molar volume of the blend component i , and q is the scattering vector. In the case of isotopic PS, V_D and V_H are nearly equal⁵, thus corrections in b or $S(q)$ are not necessary. As shown previously⁶, scattering curves obtained for blends of star and linear PS of similar molecular weight can be fit well with structure factors derived for linear chains and regularly branched n -arm stars in the incompressible random phase approximation⁷ and using a single interaction parameter. Assuming Gaussian statistics for the polymer coils in both cases, branched and linear, the measured intensity is given by

$$\frac{\left[\left(\frac{b}{V}\right)_1 - \left(\frac{b}{V}\right)_2\right]^2}{[I(q)]_{measured}} = \frac{1}{\phi_1 N_1 V_1 S_1(R_{g,1}, q)} + \frac{1}{\phi_2 N_2 V_2 S_2(R_{g,2}, q)} - \frac{2\chi}{V_0} \quad (5)$$

where V_i is the segment molar volume ($= V_2 = V_0 = 100 \text{ cm}^3/\text{mole}$), ϕ_i is the volume fraction of species i , N_i is the number of segments per chain, $(b/V)_i$ is the scattering length density for component i , and χ is the effective interaction parameter representing the strength of interaction between molecules on a per segment basis.

For the case of branched molecules, N can be expressed in terms of the number of branches N_b and the number of segments per arm, n , as $N = N_b n$. The assumption of Gaussian statistics for the arms of the stars is incorrect, but should not be a major difficulty for low numbers of arms. Stretching of the arms away from this limiting behavior increases as p increases. The structure factors for the star (S_{star}) and linear (S_{linear}) PS were obtained through brief manipulation of an expression given by Hammouda⁸:

$$S_{star} = \frac{1}{N_b} P_{11} + \frac{N_b - 1}{N_b} P_{12}, \quad (6)$$

$$S_{linear} = \frac{2(e^{-xN} - 1 + xN)}{(xN)^2}, \quad (7)$$

where

$$P_{11} = \frac{2(e^{-xn} - 1 + xn)}{(xn)^2}, \quad (8)$$

captures the intra-branch correlations,

$$P_{12} = \left(\frac{1 - e^{-xn}}{xn}\right)^2, \quad (9)$$

describes the inter-branch correlations, and $x = \frac{(qa)^2}{6}$, where a is the statistical segment length previously measured² for linear PS as $a = 6.7 \text{ \AA}$. We use the same statistical segment length for the star as well. When the value of the statistical segment length, which manifests itself predominantly in the scattering at higher values of q , is taken to have a known value, the scattering curves can be fit using the single interaction parameter, χ . Scattering was obtained for a number of star/linear PS blends as well as for two linear/linear isotopic blends of PS and a comb/linear blend of PS. In general, it was found necessary to allow for a multiplicative shift factor of order unity for all the data to provide for the degree of agreement seen in Figure 1. This correction factor accounts for random and systematic errors during measurement, including loss of intensity due to the formation of bubbles in the samples at high temperatures.

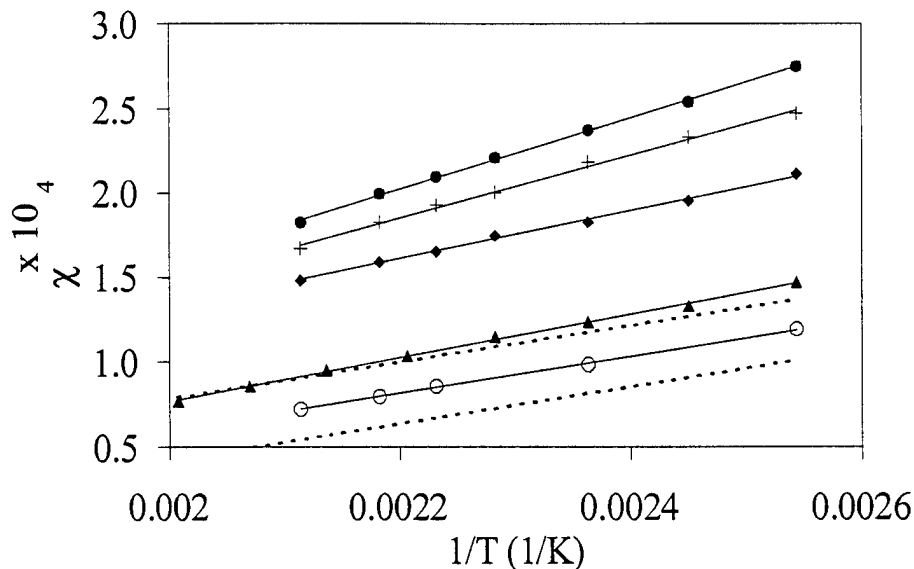


Figure 2. Interaction parameter as a function of temperature for blends containing 18 wt % of the hydrogenous PS component, be it linear or star-shaped: hPS100k (circles), h4s100k (filled triangles), h6s200k (filled diamonds), h6s100k (pluses), h8s400k (filled circles). Uncertainty bands for the linear/linear hPS/dPS blend (short dashes) corresponding to $\pm 0.2 \times 10^{-4}$ are also shown.

Values of the interaction parameter varied linearly with inverse temperature for all samples. The variations of χ with temperature for blends of hydrogenous silane linked stars in matrices of deuterated linear PS of similar molecular weight are summarized in Figure 2, for functionalities varying from four⁶ to eight. Results obtained for a blend of 18 wt % hydrogenous linear PS in a matrix of deuterated linear PS are also included for comparison. For all cases shown in Figure 2 the interaction parameters are positive and of the order of 10^{-4} , with the χ values increasing as the arm functionality of the stars increases. The results obtained for the isotopic linear/linear blend compare well with results obtained by Bates *et al.*⁵ for an isotopic linear/linear PS blend of a composition (50 vol %) and chain lengths ($N = 6.57 \times 10^3$ for the deuterated component and $N = 4.97 \times 10^3$ for the hydrogenous component) differing from ours. The estimated uncertainty of $\pm 0.2 \times 10^{-4}$ in the χ values resulting from uncertainties in the molecular weights and absolute intensity calibration is shown also. The contribution to χ due to architectural effects for the four arm star/linear blend is just large enough to be distinguished. However, for larger numbers of arms, the contribution to the interaction parameter due to architecture as compared to linear/linear blends is clear. It is apparent that there is an enthalpic contribution to χ in each case, as the curves have non-zero slope. The slope increases slightly as functionality increases.

Limitations in the determination of χ and of the contribution of architecture effects to χ arise from the precision of the molecular weight measurements and the difference in the detailed chemistry of stars *versus* the linear chains. The first issue is an important one, since the precision of the determination of such small values of χ depends sensitively on the precision of the molecular weight determinations. However, in this study molecular weights (M_n) were determined independently in at least two labs using both light scattering and gel permeation chromatography. Uncertainty in the molecular weight determinations ($\pm 3\%$) was included in the calculation of uncertainty in χ . Uncertainties in χ due to imprecision in molecular weight measurements have been mitigated in one way by using the same linear polymer in both the linear/linear blends and star/linear blends whenever

possible. The second issue, a less important one, is due to the presence of initiator fragments at the end of each arm, and the presence of a core which is chemically different from the linear chains. When structure factors incorporating these contributions were calculated for the star components, fits of the data to the Random Phase Approximation (RPA) gave rise to identical values of the interaction parameter as for the cases in which the core and chain ends were ignored. Moreover, even for the case of the largest functionality of the silane linked stars, the ratio of volumes of PS repeat units to initiator fragments was *ca.* 1000:1 while that in the eight arm star was *ca.* 4000:8. We consider this difference to be negligible in determining the value of the effective interaction parameter.

The data in Figure 2 also reveal information on the changes wrought in α_e by varying the molecular weight of the linear chain in the star/linear blend. For the case of the six arm stars two different blends with two linear chain molecular weights were made. One blend contains linear chains of M_n of 143,000 g/mol and the other blend (h6s200k) contains linear chains of M_n of 252,000 g/mol. The theory of Fredrickson *et al.*⁹ predicts that the interaction parameter should decrease as the molecular weight increases and that is what is seen here. The effect is also evident for the five arm star blend, but in a less obvious way. The five arm star blend was composed with a linear polymer having a molecular weight nearly twice that of the star. We believe that this is the reason the value of χ for the hydrogenous five arm star blend is so similar to that of the four arm star blend. If the molecular weights of the star and linear chains had been matched, the value of χ for the five arm star blend would have been markedly higher. This will be checked in future measurements.

A similar trend in χ is obtained for blends of 18 wt % deuterated silane linked star with linear PS as seen in Figure 3. The interaction parameter increases with star functionality for the case of the four and six arm star blends. The value for the d5s blend is lower than that for the d4s blend, but close to it. This underscores the fact that it is difficult to resolve the difference in χ between two cases in which the number of arms has been varied so slightly. This lack of resolution is due both to the uncertainties of the measurement and the difficulties of obtaining precisely the molecular weights

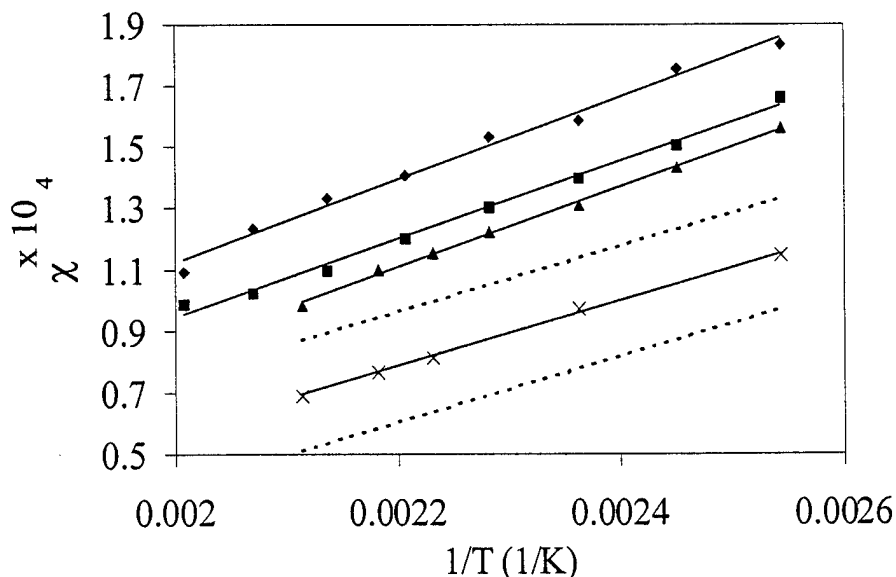


Figure 3. Interaction parameter as a function of temperature for blends containing 18 wt % of the deuterated PS component, be it linear or star-shaped: dPS100k (x), d4s100k (filled triangles), d5s200k (filled squares), d6s200k (♦). Uncertainty bands are shown illustratively for the linear/linear dPS/hPS blend (short dashes).

that provide for the most straightforward comparison. Comparison of the data for the deuterated star blends with that for the hydrogenous star blends reveals one additional interesting feature. While χ values for the blends with deuterated four and five arm stars were higher than those for the corresponding blends with hydrogenous stars, the same is not true for the six arm star blends.

The impact of blend composition on the apparent value of χ was studied using the six arm star blends. An additional measurement was made on a blend of composition 50/50. A plot of χ as a function of $1/T$ for the two blends containing 18 wt % six arm star (hydrogenous or deuterated) and for the third blend containing 50 wt % star is shown in Figure 4. When the composition of star increases from 18 to 50%, the value of χ drops about 25%.

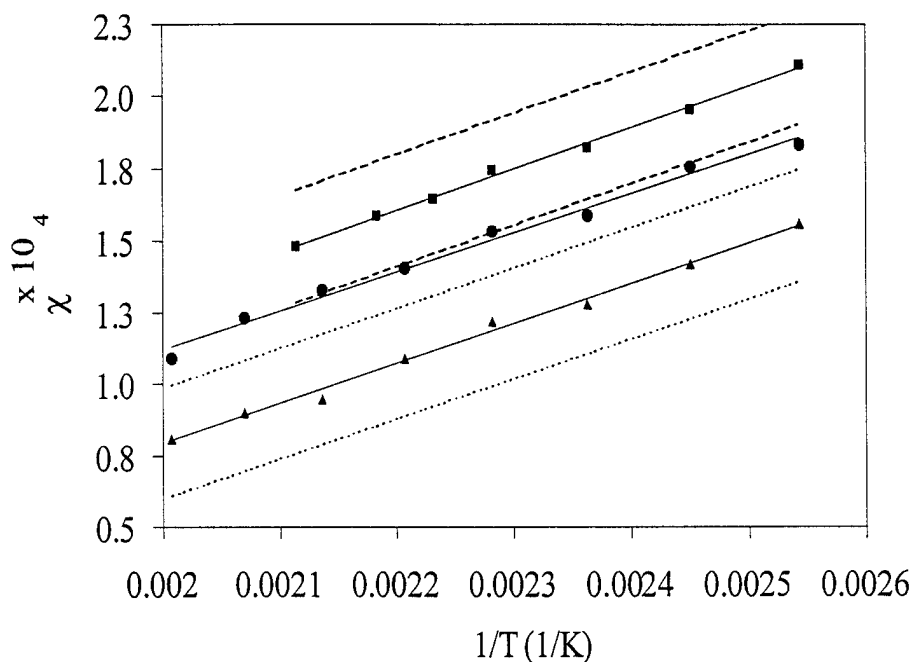


Figure 4. Interaction parameter as a function of temperature for three blends of six-arm star PS. Two blends contain 18 wt % of the deuterated [d6s200k (filled circles)] or hydrogenous [h6s200k2 (filled squares)] star and the third blend [50d6s200k (filled diamonds)] contains 50 wt % of the deuterated star. Uncertainty bands are shown for the h6s200k2 blend (long dashes) and the 50d6s200k blend (short dashes).

This drop in χ is in good agreement with the behavior anticipated from the theory of Fredrickson and coworkers⁹. In their treatment, which ignores labeling effects, changing the composition of star from 18 to 50% is predicted to cause a drop in χ of about 40%. The drop in our data is smaller, but the difference can be quantitatively accounted for simply by considering the effect of labeling. Londono *et al.*¹⁰ have shown that in linear/linear isotopic blends of PS increasing the composition of one component from 18 to 50% leads to an *increase* in χ of about 15%. If one imagines that the architecture effect and labeling effect are approximately additive, a net decrease of 25% would be expected when changing the composition of the star/linear blend from 18 to 50%. This is in very good agreement with the experimental result¹⁰. Also this limited data on the composition dependence of χ in the star/linear blend suggests that the effect of architecture on the

interaction parameter is stronger than the effect of labeling. Certainly additional star/linear blend compositions need to be measured to further clarify the phenomenon.

To investigate the effect that further increases in functionality have on χ , blends of stars linked with DVB were studied. Properly comparing the results obtained for the two types of star/linear blends requires that two distinctions be made. First, the DVB linked stars are not only characterized by larger numbers of arms, but also by cores that are chemically different from the cores of the silane linked stars. The DVB cores are chemically more similar to the PS arms than are the silane cores. However, the DVB cores are larger and less well-defined than are the silane based cores. Second, the functionality is not as narrowly defined for the DVB linked stars. In spite of these differences, the results obtained for the interaction parameters follow the same general trend as seen for the silane linked stars. That is, χ increases with star functionality as shown in Figure 5. The interaction parameters for the blends with DVB linked stars are higher than those for the blends with silane linked stars. The blend containing the hydrogenous 12 arm DVB linked star is characterized by an interaction parameter twice that obtained for the blend containing the hydrogenous eight arm star. In contrast to the behavior seen for the silane linked stars, here the effect of swapping the labeling is unmistakable. When the branched chain is deuterated the value of χ is much larger. The effect is in the same direction as that seen for short branched polyolefin blends^{11,12} and isotopic polydiene blends¹³. The magnitude of the difference is much larger, however, for our blends of DVB-linked stars.

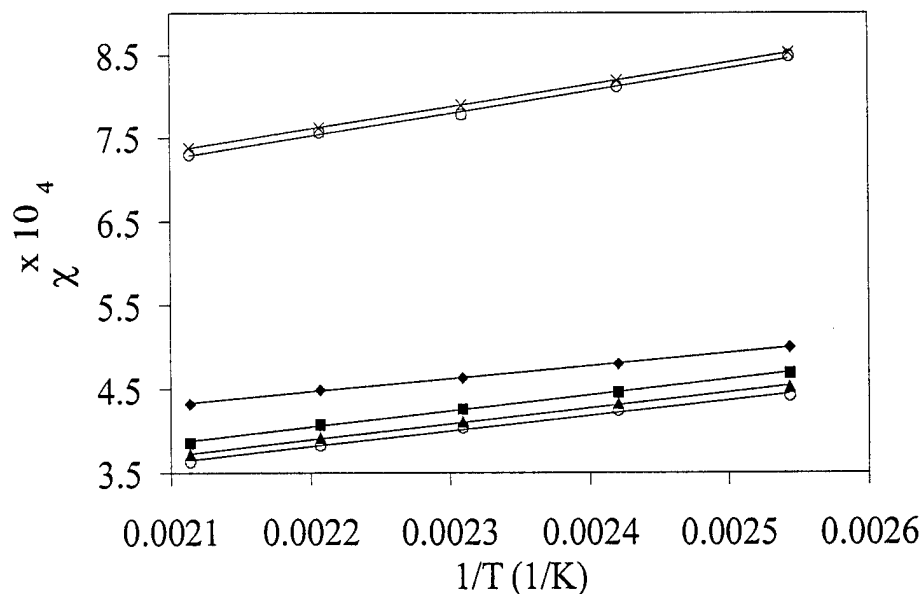


Figure 5. Interaction parameter as a function of temperature for blends of DVB-linked PS star/linear PS blends for both labeling schemes (18 wt % hPS and 18 wt % dPS) and various functionalities: hDVB12 (circles), hDVB14 (filled triangles), hDVB17 (filled squares), hDVB21 (◆), dDVB15 (○), dDVB16 (×).

For purposes of quantitative comparison among the different blends and with the theory of Fredrickson and coworkers⁹ Table 3 summarizes the experimentally determined values of χ at 220 °C for each blend. For the four, five, and six arm stars, for which we have hydrogenous and deuterated analogs that are reasonably well matched, one may calculate a χ averaged between the two labeling

schemes and this is the value that is given. A comparison between this average and the theory seems most prudent since the theory has no means by which to account for labeling differences. For the DVB linked stars, no two blends are similar enough in both functionality and arm size to perform such an average reasonably. Included in the table as well are theoretical values for the entropic contribution to χ predicted using the universal approximate expression [eqn (3) above] given by Fredrickson *et al.*⁹. This theoretical value accounts not only for the differences in functionality among the various blends, but also for variations in sizes of the arms from blend to blend. A closer comparison may be attempted using a more detailed expression (eqn 3.15 in reference 9) given by those authors. That expression accounts additionally for the effect of changing the size of the linear chain, but requires computing a cutoff length for which no exact expression is given in Ref. 9. The third quantity tabulated is $\Delta\chi$, the difference between the experimental value of χ for a given star/linear blend and the value measured for the linear/linear isotopic blend. $\Delta\chi$ is an estimate of the architectural contribution to χ for that blend. Thus comparison should be made between $\Delta\chi$ and the theoretical predictions, keeping in mind that the theoretical values are for an athermal blend and we have taken liberties in appropriating the theory for comparison with blends containing stars with small numbers of arms. To our knowledge there is no published theory including enthalpic effects to which one could compare.

Table 3. Interaction parameter values measured at 220 °C for a series of PS isotopic blends

Blend	χ at 220 °C (x 10 ⁻⁵)	$\Delta\chi^b$ (x 10 ⁻⁵)	Theoretical architecture contribution (x 10 ⁻⁵)
linear/linear	6	0	
4 arm star/linear	9 ^a	3	2
5 arm star/linear	9 ^a	3	5
6 arm star/linear	13 ^a	7	8
h 8 arm star/linear	17	11	8
h 12 arm star/linear	35	29	16
h 14 arm star/linear	36	30	9
d 15 arm star/linear	71	65	22
d 16 arm star/linear	71	65	30
h 17 arm star/linear	37	31	31
h 21 arm star/linear	42	36	9

^a Averages of χ between labeling schemes (defined in the text).

^b Difference between the experimental value of χ for a given blend and the value measured for the linear/linear isotopic blend (defined in the text).

For the silane linked stars, which have smaller numbers of arms, the experimentally estimated contributions to χ due to architectural effects are similar in magnitude to the predicted values. For the DVB linked stars the experimental value is markedly higher in all but one case. One also sees that while the experimentally determined χ values simply increase monotonically with star functionality, (using only h-DVB or d-DVB stars for the comparison) the theoretical values do not. This is due to the fact that arm size varies through the series of polymers. If the effect of arm size were to have the relative importance predicted by the theory one would have expected very similar experimental χ values for the blends of the six and eight arm silane linked stars, due to the much larger arms on the eight arm star. Also the experimentally observed χ values for the blends with DVB linked stars should have fallen in a different order, for example, with the χ value for the blend containing the 14 arm star lying substantially below that for the blend with the 12 arm star. Further study with appropriately chosen star materials can address the relative importance of the variation in arm size. It is important to note that even in the face of these discrepancies between the theory and experimental results an important prediction of the study by Fredrickson *et al.*⁹ is confirmed. The general magnitude of the effect predicted for stars is correct. Thus, interactions due to architecture alone are insufficient to lead to bulk phase separation for star/linear blends over a wide range of molecular weight and number of arms.

Consideration of the data from the comb/linear blend suggests that another prediction of the theory⁹ is correct. The effect of architecture on χ is much larger when the branched polymer is a comb. The values of effective χ for the six arm comb/linear blend (Figure 6) are more than 20 times higher than the values seen for the six arm star/linear blends. This comparison is not as rigorous as that among the various star/linear blends, since the comb is less well-defined and differs chemically from the star. Further work is underway to provide a more precise comparison. We note that with the size of interaction seen in the comb/linear blend one is approaching that for which one would

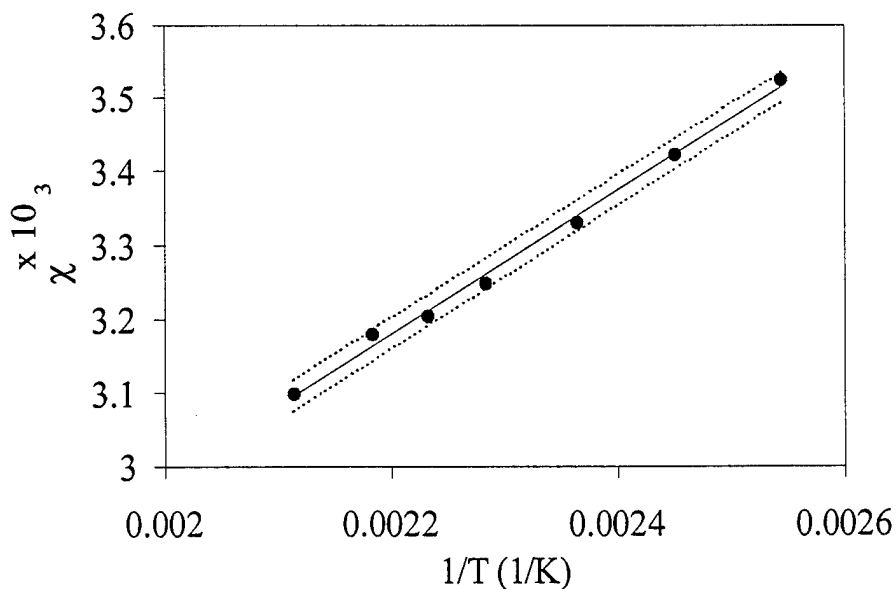


Figure 6. Interaction parameter as a function of temperature for the comb/linear PS blend containing 18 wt % h6-branch PS comb in a matrix of deuterated linear PS of symmetric molecular weight. An estimate of the uncertainty is shown with short dashes.

expect a 50/50 blend to bulk phase separate at the temperatures studied here. A naive estimate of the critical value of χ for this blend, using the Flory approximation for a symmetric linear blend ($\chi_c = 2/N$), is 0.003. This suggests that if the composition of comb were increased up to 50% phase separation would be seen.

Polybutadiene blends

For a better appreciation of the work from the entire award period we summarize also the results on bulk thermodynamic interactions in blends of star and linear PB presented in last year's report. The preparation of the samples and the manner of measurement were similar to those for the polystyrene samples. The PB samples did not have to be pressed, however.

The values measured for the interaction parameters appear in Figure 7. For this plot χ has specifically been calculated using the same value of segment volume as for the case of polystyrene to make for easier comparison. To provide base line information first an isotopic linear/linear blend was studied. The magnitude of χ seen in these measurements at temperatures from 40 to 160°C was consistent with results from Bates *et al.*¹⁴, though the change with temperature seen in our measurements was somewhat greater. It should be noted, however, that Bates studied a different molecular weight and the component molecular weights were strongly asymmetric in his case.

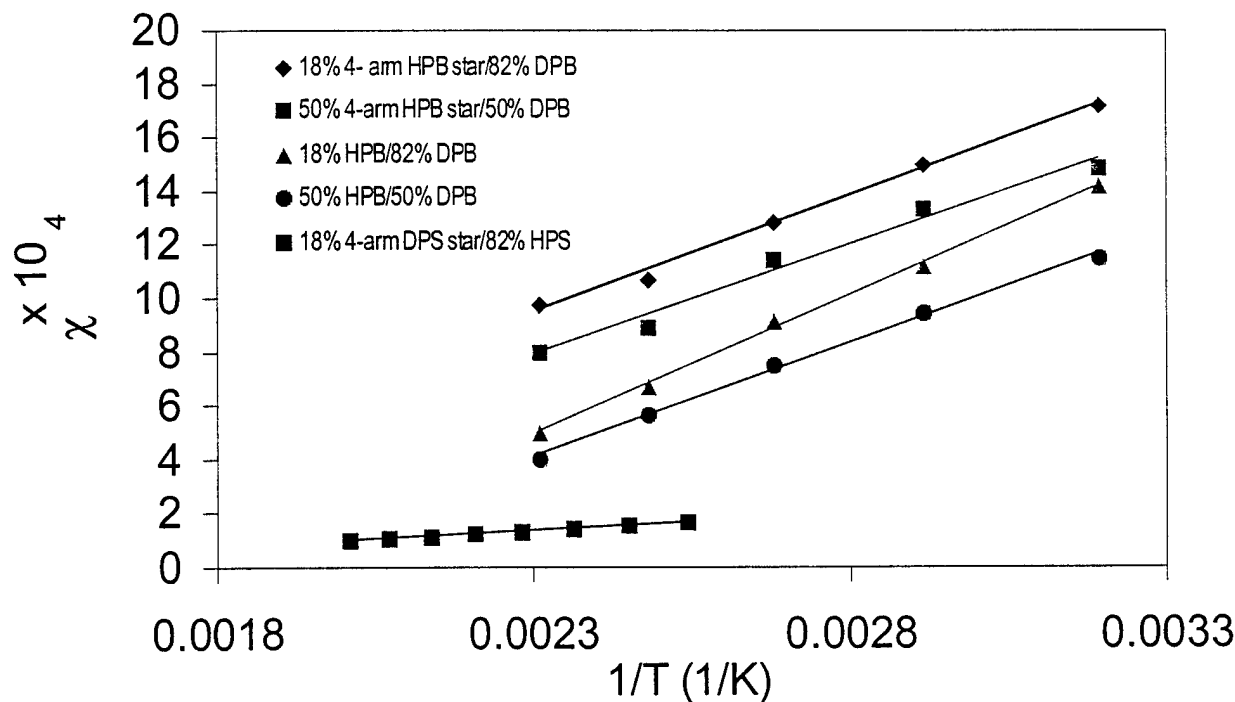


Figure 7. Temperature dependence of the thermodynamic interaction parameter, χ , for polybutadiene blends, where χ is calculated using the same segment volume as used for the PS blends above. The blends are identified in the legend, which also gives equations corresponding to the linear fits. For comparison the data for the blend of 18% four arm dPS in linear PS is shown as the curve at the bottom of the plot. The temperature ranges over which the measurements were made do not match due to the different T_g s of the two polymers and the greater sensitivity of PB to thermal degradation.

We also studied two compositions of linear/linear PB blends, 18% hPB and 50% hPB, and two compositions of star/linear PB blends. We observed a dependence of χ on composition for the linear/linear blends as others have for various polymers. The subtle difference of temperature dependence with composition suggested by the data is not large enough to be significant. Variation in the value of χ with blend composition was also found for the star/linear blend, with the strength of the composition dependence being roughly the same as that seen for the linear/linear blend. χ measured for the composition of 18% is higher in both cases. The values of χ found for a blend of 50% four arm hPB star in linear dPB lie consistently above those found for the linear/linear isotopic blend of either composition, suggesting the presence of a real architectural effect even after considering the errors on the determination of χ , which we estimate preliminarily to be of order 20%. Since the star/linear blend with deuterated star has not yet been measured it is not possible to estimate the interaction parameter just due to architecture by averaging over two labeling schemes as was done for the polystyrene four arm star/linear blend above.

Nonetheless we can compare the strengths of the isotopic effect and architecture effect in the PB and PS blends and the pertinent values are summarized in Table 4. The magnitude of χ for the PB linear/linear blends due to the isotopic effect is roughly *six times* higher than that for the PS linear/linear blends once one has normalized to a common segment volume of 100 cm³/mole. However, the apparent bulk architectural effect for a four arm star/linear blend (considering only one labeling scheme, i.e. deuteration on the linear component) is about *20 times* higher for the PB blends. This may be contrasted with the PS blends where the absolute magnitude of the architecture effect is less than the magnitude of the isotopic effect in the case of the four arm star blend. Thus, to the extent that bulk behavior drives surface behavior, we would expect to see stronger surface segregation of stars in the PB blends (see section III below).

Table 4. Comparison of Magnitudes of the Isotopic and Architecture Effects at 160°C

Blend type	χ	$\Delta\chi$ (architecture) = $\chi(\text{star/dlinear}) - \chi(\text{linear/dlinear})$
18 % linear PS/linear dPS	1×10^{-4}	-
18 % linear PB/linear dPB	6×10^{-4}	-
18 % 4 arm PS/linear dPS		2×10^{-5}
18 % 4 arm PB/linear dPB		40×10^{-5}

Conclusions from Measurements of Thermodynamic Interaction in the Bulk

For each polystyrene blend the contribution due to architectural effects alone can be estimated by comparison with the interaction due to isotopic labeling alone seen in a linear/linear isotopic blend. This contribution due to architectural differences can be quantified as such without making any assertions as to whether it is entropic or enthalpic in origin. However, it is striking to find that it is similar in magnitude to the "entropic" contribution predicted by the theory of Fredrickson *et al.*⁹ for an athermal blend. Thus the theory's assertion that bulk phase segregation is unlikely for blends of linear chains with stars is substantiated⁹.

A clear trend of χ increasing with star functionality is seen for this series of stars, even though theory would suggest that variations in arm size should lead to variations in χ which are not simply

monotonic in number of arms. Agreement with theoretical expectations is seen on two other points, though. First, the variation in χ with composition of the star/linear blend predicted by the theory is seen experimentally, though more compositions should be measured to test this more fully. Second, the interaction between a comb branched chain and its linear analog is much stronger than that between a linear analog and a star with the same number of arms as the comb.

The isotopic effect is about six times stronger in PB blends. A first estimate suggests the bulk architectural effect in a PB star/linear blends is 20 times stronger than the isotopic effect. That is the relative strength of the architectural effect in the bulk is much larger for PB blends than for PS blends.

III. SURFACE SEGREGATION IN BLENDS OF BRANCHED AND LINEAR POLYMERS

In the second component of the work surface segregation in the blends of long branched and linear materials was considered. This final year results for polystyrene systems from dynamics secondary ion mass spectroscopy, neutron reflectometry, and nuclear reaction analysis measurements were analyzed. Also polybutadiene blends were investigated. All the work with polystyrene blends is discussed first and then the polybutadiene investigation is presented.

Surface Segregation in Polystyrene Blends

Sample Preparation. Blends containing 18 wt % star (either hydrogenous or deuterated) with 82 wt % of the contrasting linear analog were prepared by dissolving the polymers in toluene. The solutions were filtered three times using 0.45 μm pore size nylon filters. Thin polymer films were obtained by spin casting the filtered solutions onto clean, polished silicon wafers (purchased from Semiconductor Processing). The wafers were cleaned by immersing in "piranha" solution for 30 minutes at 60 – 90 °C. (*Piranha is a 7:3 mixture of H_2SO_4 : H_2O_2 obtained by adding the peroxide to the acid. The acidic solution is dangerous to work with and must be handled in the hood at all times and with acid resistant gloves.*) They were then washed in deionized water for 30 minutes, and blown dry with N_2 . Films of thicknesses varying from 800 to 1110 Å were cast by spinning for two minutes at 2000 rpm. Four inch diameter wafers were used for neutron reflectometry (NR) measurements, while for dynamic secondary ion mass spectroscopy (DSIMS) and nuclear reaction analysis (NRA) one inch diameter wafers were used. Film thicknesses were measured using ellipsometry and, in some cases, X-ray reflectometry as well. Samples were annealed under high vacuum (10^{-6} Torr) for 7.4 days, at 170–180 °C. After annealing, samples were rapidly quenched (rate of 25 °C/min) to temperatures well below the glass transition temperature of PS (100 °C), so as to prevent any motion of the polymer chains that would result in a change in the composition profile. A summary of the samples investigated and the nomenclature used is provided in Table 5. The abbreviation used to name a star polymer is also used to refer to the blend containing that star, where the context should make clear whether the homopolymer or its blend is being considered.

In order to ensure that no thermal degradation occurred in the samples, a high vacuum oven was used for annealing. GPC measurements were performed on samples annealed under roughing vacuum and high vacuum for two to eight days for comparison. Significant chain degradation was observed after only two days of annealing under roughing vacuum while in the case of the high vacuum annealing there was no indication of thermal degradation of the chains even after eight days.

Table 5. Blend Nomenclature and Composition, Molecular Weight of Components

<i>Blend</i>	<i>18 wt% PS Star Component</i>	<i>PS Linear Component</i>
h4s	h4-arm silane-linked, 85k	dPS143
h5s	h5-arm silane-linked, 131k	dPS252
h6s	h6-arm silane-linked, 161k	dPS252
d4s	d4-arm silane-linked, 100k	hPS132
d5s	d5-arm silane-linked, 164k	hPS132
d6s	d6-arm silane-linked 157k	hPS230
hDVB14s	d14-arm DVB-linked, 290k	dPS252
dDVB15s	h15-arm DVB-linked, 200k	hPS212

Measurements. Neutron reflectometry measurements were performed on the reflectometer NG1 at the Cold Neutron Research Facility of the National Institute for Standards and Technology in Gaithersburg, Maryland. A neutron beam of wavelength, λ , of 4.75 Å with a resolution of $\Delta\lambda/\lambda$ of 0.015 was used. Specular reflectivity was measured over a q range of 0 – 0.25 Å⁻¹ using gradually increasing slit sizes in order to collect data with approximately constant relative resolution in q ($\Delta q/q$). Transverse scans were performed for a number of samples in order to survey the off-specular and diffuse scattering. This was done by varying the incident angle with respect to the surface, θ , while keeping 2θ fixed at 4° and 10°, respectively. Background scattering was also measured on each side of the specular and the background under the specular intensity estimated by linear interpolation. Reflectivities were obtained by subtracting the background from the raw reflected intensities and then dividing by the main beam intensity at each value of q . Inferences about a sample's composition depth profile were drawn by seeking parameter values which provided "best fits" between a likely candidate composition profile and the experimental data. Details of the fitting procedure are given elsewhere¹⁵. While this parameter estimation approach is nonunique, complementing the NR analysis with measurements using the techniques of DSIMS and NRA, which directly yield composition profiles, ensured that the profiles found from the NR data were realistic.

Dynamic Secondary Ion Mass Spectroscopy measurements were carried out at the MatNet Center for Analysis of Materials at Case Western Reserve University. A PHI660 Scanning Auger Microprobe System combined with a PHI3600 Secondary Ion Mass Spectrometer were used to obtain the depth profiles. An incident beam of 2 kV Ar⁺ oriented at about 40° with respect to the sample's normal was utilized to sputter the sample, probing thicknesses between 0 and 1100 Å with good depth resolution. Penetration of the sample from the surface to a certain predetermined depth was obtained by rastering the incident primary ion beam over a designated area with width and length each several times the beam focal width, creating a flat bottomed crater. Additional sample preparation was needed in the case of DSIMS measurements. The annealed and unannealed samples were capped with sacrificial layers of PS of about 200 Å in thickness, to ensure that the sputtering rate came to a steady state before the sample proper was reached. Each polymer "sandwich" was coated with a layer of gold (*ca.* 50-100 Å) to prevent sample charging. DSIMS measurements were conducted under high vacuum. Selected positive and negative ions, H⁻, D⁻, CH⁻, CD⁻, O⁻, C⁺, and Si⁺, were

monitored at a sputter rate of about 5Å/min and mass analyzed as a function of charge/ mass ratio. Counting times of 1 to 3.5 seconds were used for each species. DSIMS yields directly a relative composition depth profile when an appropriate ratio of yields is plotted as a function of sputter time since sputter time is proportional to depth. Actual compositions were obtained by scaling using the known overall sample composition and the imposition of a species mass balance. Sputter time was converted to depth assuming a steady etch rate. The resulting profile represents the true composition profile convoluted with a depth dependent resolution function. At the sample surface the resolution is about 130 Å full width at half maximum (FWHM).

Nuclear Reaction Analysis with a resonant reaction was the third method used to quantify the surface segregation in these blends of star and linear chains. NRA is a direct ion beam technique, which allows depth profiling of thin polymer films with a higher resolution than does DSIMS (4 nm at the film surface and 10 – 15 nm at a depth of 100 nm into the film). Measurements were performed at the Army Research Laboratory in Aberdeen, Maryland. NRA with resonant reaction is a specific type of NRA which may be distinguished from the nonresonant NRA with ^3He which has been used more widely with polymers¹⁶. This NRA technique is based^{17,18} on the resonant nuclear reaction $^1\text{H}(^{15}\text{N}, \alpha, \gamma)^{12}\text{C}$ which occurs when the energy of an incident ^{15}N beam equals the resonant energy, E , of 6.4 MeV. The ^{15}N beam is incident on the sample under an angle of 90° from the surface and the resulting 4.43 MeV gamma rays are detected at an angle of 90° as well. The yield of gamma rays is proportional to the amount of hydrogen present at the depth at which the resonant reaction occurs. The energy of the incident beam can be increased step by step, from 6.4 to 8 MeV, allowing for the reaction to occur at progressively larger depths in the sample. In this manner, concentration profiles of hydrogen as a function of depth can be obtained. NRA also yields the composition profile directly, with a resolution at the surface (*ca.* 80 Å) better than that of DSIMS.

Results and Discussion

a) Silane-linked star/linear blends

We consider first the quantification of the surface segregation in a star/linear blend in the case of the silane coupled stars which are better defined in functionality. Since NR is more highly resolving, these results are highlighted; however their interpretation must be consistent with information from the DSIMS and NRA measurements. When the star was deuterated, both the isotopic and architectural effects were expected to drive segregation of the star to the surface. Thus blends of this type were studied first. DSIMS results for blends of six arm deuterated stars with hydrogenous linear analogs are shown in Figure 8, for the annealed and the unannealed cases. As expected, the resolution of the step function in concentration at the surface is better than that at the substrate interface. A number of observations may be made on the basis of these data alone. First and foremost, the surface excess, which can be appraised directly from DSIMS data, is modest in size (surface excess value at the air interface of 5 ± 2 Å and at the substrate interface of 8 ± 2 Å)¹⁹. Secondly, the segregation is seen over a length scale commensurate with the R_g 's of the polymers, about 100Å, but the form of the profile on this length scale cannot be resolved by DSIMS. NR measurements are needed to do this. Thirdly, the preferential segregation of the star to *both* the air and substrate interfaces is seen, with the segregation to the substrate being stronger. The chemical natures of the two media adjoining the blends at the interfaces are very different, but both present 'hard walls' in some sense. If the segregation were driven purely by chemical interactions the amount segregated to the two interfaces should be very different. This is not the case. On the other hand, if the segregation were only entropic in nature one might expect very similar segregation to both interfaces. This is also not the case. The chemistries of the adjoining media play some role. In fact, it is known from studies of linear isotopic blends²⁰ that deuterated linear PS chains tend to segregate to the silicon oxide surface. If the oxide is removed²⁰ the segregation of deuterated material to that

interface is diminished. It is then reasonable to suppose that the enhancement at the substrate is due in part to the interaction between the deuterated PS and the silicon oxide.

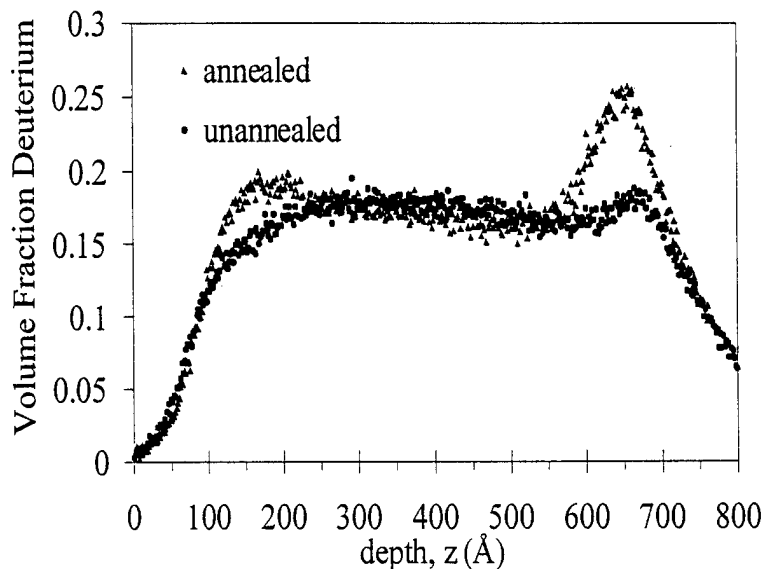


Figure 8. DSIMS data for annealed (filled triangles) and unannealed (filled circles) films of 18 wt % deuterated six arm PS star in hydrogenous linear PS. Annealing was conducted under high vacuum (10^{-6} Torr) for 8.4 days at 180 °C. Upon annealing the deuterated star is seen to segregate to both interfaces, with a higher amount of deuterated material at the substrate interface.

DSIMS data for the blend with deuterated four arm star (not shown here) presented a puzzle. No segregation was seen at the surface. The correlation length for segregation should be of order of the radius of gyration of the star, which for the four arm star is 69 Å. Since this is smaller than the resolution of DSIMS at the surface, *ca.* 130 Å, the absence of evidence of segregation could simply be due to a lack of resolution. Measurements with NR and NRA were necessary to resolve this issue.

The concentration profile measured by NRA for the deuterated four arm star/linear blend is shown in Figure 9. As in the case of DSIMS, no segregation of the star can be seen at the air surface. Due to the decreasing resolution as the depth increases and due to the relatively small sizes of the linear and star chains, the measurement is not able to capture the behavior of the blend at the substrate interface. However, both DSIMS and NRA indicate that there is no preferential segregation of star material at the air surface.

Figure 10 presents the NR data for the d4s, d5s and d6s samples, while the corresponding volume fraction profiles are presented in Figure 4. Regions of higher scattering length density, b/V , correspond to regions enriched in deuterium. The interfacial excesses derived from these profiles are given in Table 3. In order to understand how the composition profiles shown in Figure 11 are obtained from the NR data it is necessary to consider the interpretation of the NR data. The success with which the form of the NR data was captured with model "fits" varied somewhat from sample to sample as a result of film dewetting. The dewetting is difficult to avoid, progresses with annealing time, and leads to a loss of detail (i.e. interference fringes) in the curves at higher values of q . Since the important details of the surface segregation profile manifest themselves most prominently in that

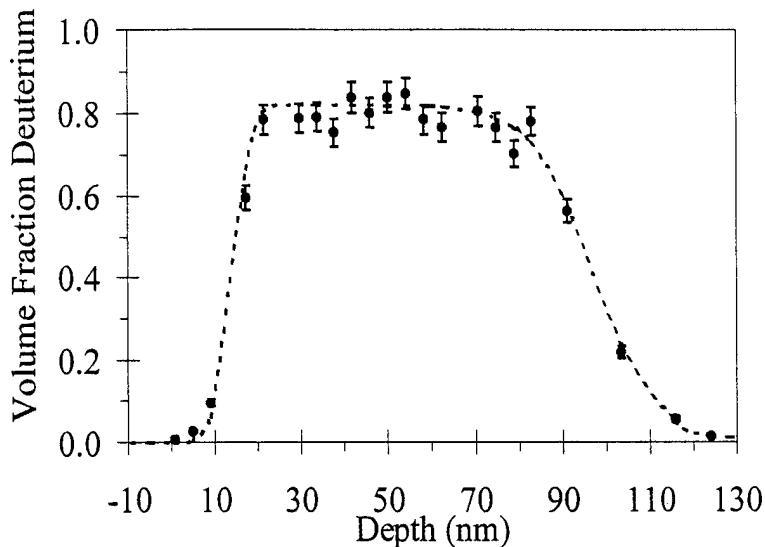


Figure 9. Depth profile obtained for an annealed (filled circles) blend of 18 wt% deuterated four arm PS star in hydrogenous linear PS obtained with NRA. The continuous line is used just as a guide to the eye. The unannealed profile (---) is simulated using a tanh function. Annealing was conducted under high vacuum (10^{-6} Torr) for 8.4 days at 180 °C.

part of the curve at q just above the critical value of q , modeling focused on providing a good representation of the data there. The overall level of the reflectivity at higher values of q reflects both the sample roughness and the sizes of “jumps” in scattering length density at the interfaces at the top and bottom of the film. Composition profiles determined in this way from the NR cannot stand on their own, but must be consistent with the independent information obtained from NRA and DSIMS.

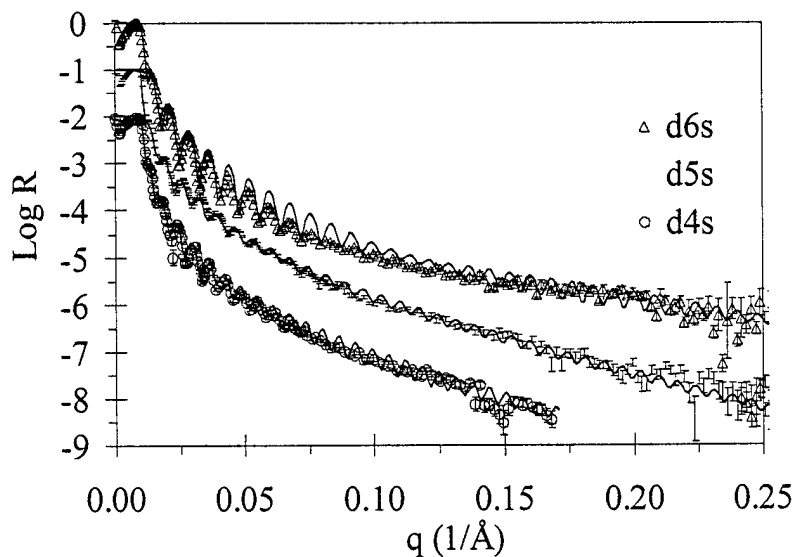


Figure 10. NR corrected data and fits obtained for thin films of annealed d4s (circles), d5s (\square) and d6s (Δ) blends. Annealing was conducted under high vacuum (10^{-6} Torr) for 8.4 days at 180 °C. The reflectivity curves are offset by a factor of 10.

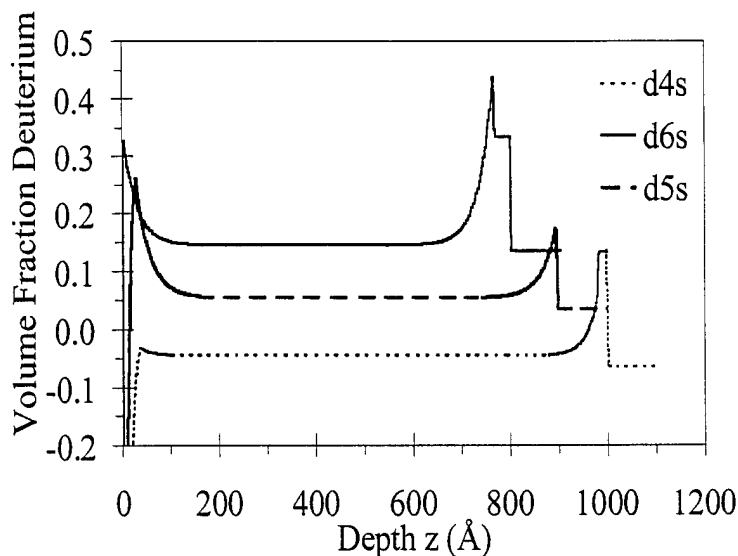
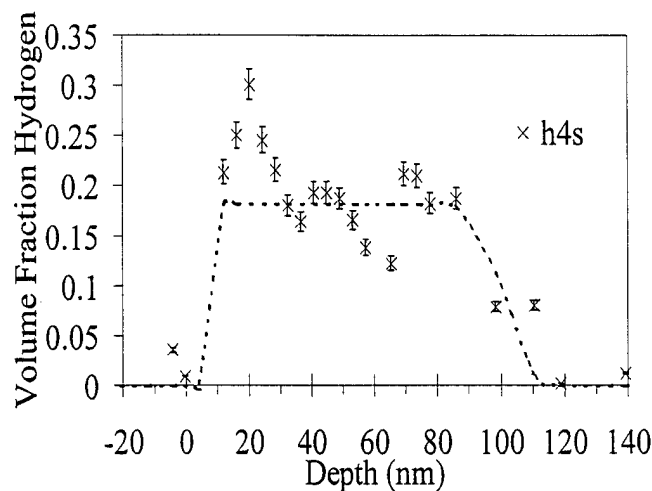


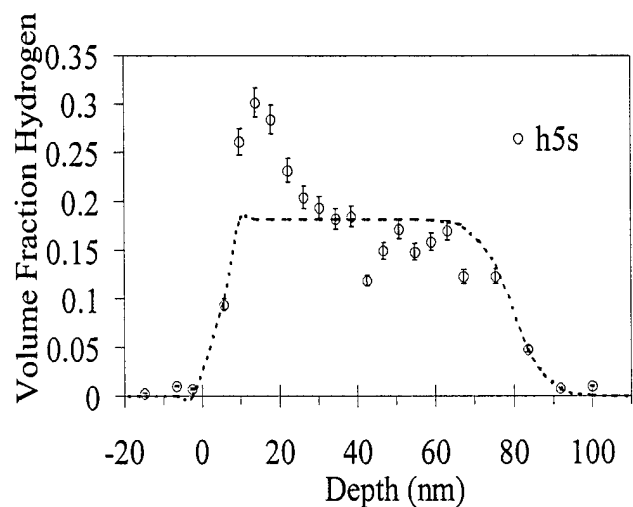
Figure 11. Depth profiles for annealed d4s (\cdots), d5s ($---$) and d6s (solid curve) blends corresponding to the reflectivity fits shown in Figure 10. The profiles are offset by a factor of 10. Deuterated star material is present at both interfaces with the amount at the silicon oxide interface being higher for the four and six arm star blend. In the case of the five arm star blend the amount of star at the air surface is higher (no oxide layer on the substrate). The overall amount of deuterated star segregated is seen to increase as the number of arms increases.

The NR measurement confirms that in the case of the deuterated four arm star/linear blend there is no significant segregation of the star at the air surface, and only a small excess at the substrate interface. For the five arm star film, which was deposited on an etched wafer (no native silicon oxide layer present), both the air and the substrate are enriched with deuterated star material, with the air interface excess being higher. This is consistent with the argument that chemistry plays a role in determining the magnitude of the interface segregation. When the silicon oxide layer is present, as in the case of the d6s blend, the amount of star segregated at the substrate interface is higher than that seen at the air interface. Taken all together the data for the four, five, and six arm stars are consistent with an increase in surface excess with number of arms, but the trend can be specified no further than that. We must note that in the case of the d6s blend the molecular weight of the linear matrix is nearly twice that in the case of the d5s blend and the introduction of this additional variable precludes specifying the trend more precisely. Since annealing was conducted under the same conditions and for the same amount of time, it is possible that the d5s blend was closer to equilibrium. Additional DSIMS data, for the d6s blend which show an increased surface excess (9 Å) upon annealing for an extra day, support this hypothesis.

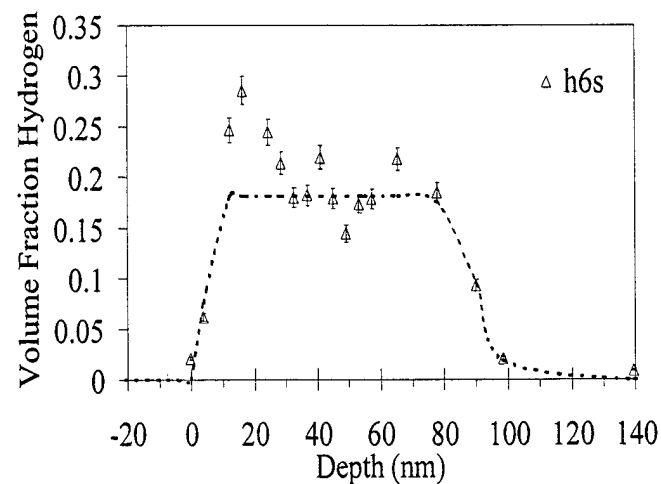
In order to distinguish between the effect of deuteration on the preferential segregation of star material and that of architecture, surface measurements were performed on blends of hydrogenous star/deuterated linear PS. NRA results show star segregation at both the air and the substrate interface for four (Figure 5a), five (Figure 5b), and six (Figure 5c) arm hydrogenous star blends. In this case, in contrast with blends containing deuterated stars, the amount of star segregated at the air interface is higher than that at the substrate, for all three blends studied. In addition, surface excess of star at the air interface is seen to increase slightly as the number of arms increases from four, to five,



a.)



b.)



c.)

Figure 12. NRA depth profiles obtained for annealed films of a.) h4s (x), b.) h5s (circles) and c.) h6s (Δ) blends. Annealing was conducted under high vacuum (10^{-6} Torr) for 8.4 days at 180 °C. The unannealed profiles (---) are simulated with *tanh* functions to describe the interfaces. NRA results indicate segregation of hydrogenous star material at the air surface and are supported by NR results (Figures 13 and 14).

and then to six. This is qualitatively consistent with theoretical results obtained by Wu and Fredrickson²¹ which predict an increase in the amount of star segregated at the surface as the number of arms increases for blends in which the overall molecular weights of the components are comparable.

The NRA results are supported by NR findings. Figure 13 summarizes the NR results obtained from the hydrogenous silane-linked star/deuterated linear thin films (h6s, h5s, and h4s blends). Figure 14 shows the corresponding volume fraction profiles estimated by fitting. The surface excess values calculated from the two types of data compare well for the air surface. Although the depth resolution of NRA (70 Å – 150 Å) is inferior to that of NR (10 Å), the advantage of using NRA is that no fitting is necessary to obtain depth profiles. NR data indicate that the amount of star at the air interface increases very slightly as the number of arms is increased. To check the significance of the small differences seen in the surface excess values, we attempted to fit the data for the h6s blend with the models used for the h5s and h4s blends (accounting for the overall film thicknesses). The h5s and the h4s segregation profiles gave significantly poorer agreement with the h6s reflectivity data.

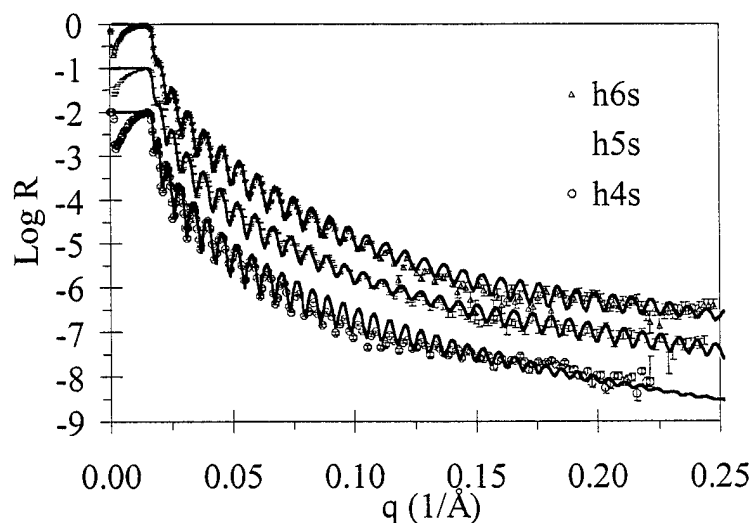


Figure 13. NR corrected data and fits obtained for thin films of annealed h4s (circles), h5s (only error bars) and h6s (Δ) blends. Annealing was conducted under high vacuum (10^{-6} Torr) for 8.4 days at 180 °C. The reflectivity curves are offset by a factor of 10.

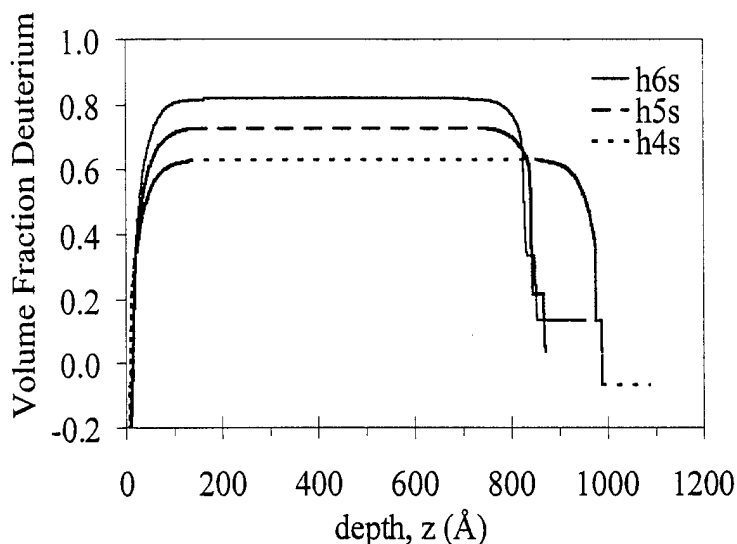


Figure 14. Depth profiles for annealed h4s (\cdots), h5s ($---$) and h6s (solid curve) blends corresponding to the reflectivity fits shown in Figure 13. The profiles are offset by a factor of 10. Hydrogenous star material is present at both interfaces with the amount at the air surface being higher than at the substrate (silicon oxide) interface for all blends. The amount of hydrogenous star segregated at the air surface is seen to increase as the number of arms increases.

b) DVB-linked star/linear blends

In order to explore systems in which the functionality of the stars was higher, samples consisting of branched components that were DVB-linked stars were studied. The DVB-linked stars are discussed separately, because in addition to having more arms, the character of their cores differs somewhat from that of the silane-linked stars. For the DVB-linked stars the functionality is not as narrowly defined and the cores are larger and less well-defined. In fact, depending on precisely how the DVB polymerizes it is possible for the DVB-linked chain to look like a comb polymer with a very short backbone and very dense attachment of side chains. For that reason one may even wish to consider the DVB-linked chains as having a topological character between those of well-defined stars and well-defined combs. The NR results obtained for the dDVB15s and hDVB14s blends are shown in Figures 15 and 16, respectively. Composition profiles are shown in the insets together with plots of the scattering length density (b/V) as a function of depth.

Annealing for the DVB blend samples was conducted under high vacuum at 180 °C, but only for 7.4 days as opposed to 8.4 days in the case of the silane-linked star blends. Preferential segregation of star material at both interfaces is seen for the two DVB star/linear blends. As in the case of the d6s and d4s blends, the substrate has its native oxide. The excess of star seen at the silicon oxide substrate ($41 \pm 1 \text{ \AA}$) interface for the dDVB15s blend is large in comparison to the excess at the air interface ($12 \pm 1 \text{ \AA}$). In comparison to the other two deuterated star/hydrogenous linear blends presented here (d4s and d6s), the amount of star material at the substrate interface increased dramatically for the DVB-linked stars ($41 \pm 1 \text{ \AA}$ for the dDVB15s blend *versus* $9 \pm 1 \text{ \AA}$ for the d6s blends and $3 \pm 1 \text{ \AA}$ for the d4s blend). The sample with the blend containing the hDVB14s presents as nearly as possible the case with swapped isotopic labeling in order to look for the effect of the labeling. The star, in this case hydrogenous, had a functionality of 14 (hDVB14s blend). The thin film was prepared on silicon oxide. NR measurements revealed similar excesses of the hydrogenous star at both interfaces ($13 \pm 1 \text{ \AA}$ at the air surface and $10 \pm 1 \text{ \AA}$ at the substrate

interface). When compared to silane-linked hydrogenous star blends the overall amount of DVB star segregated is comparable ($23 \pm 1 \text{ \AA}$ versus $22 \pm 1 \text{ \AA}$). The trend of increasing surface excess seen as the number of arms changes from four to five to six does not extend to the hDVB14s blend, for which the surface excess value was expected to be higher than that measured for the h6s blend ($15 \pm 1 \text{ \AA}$).

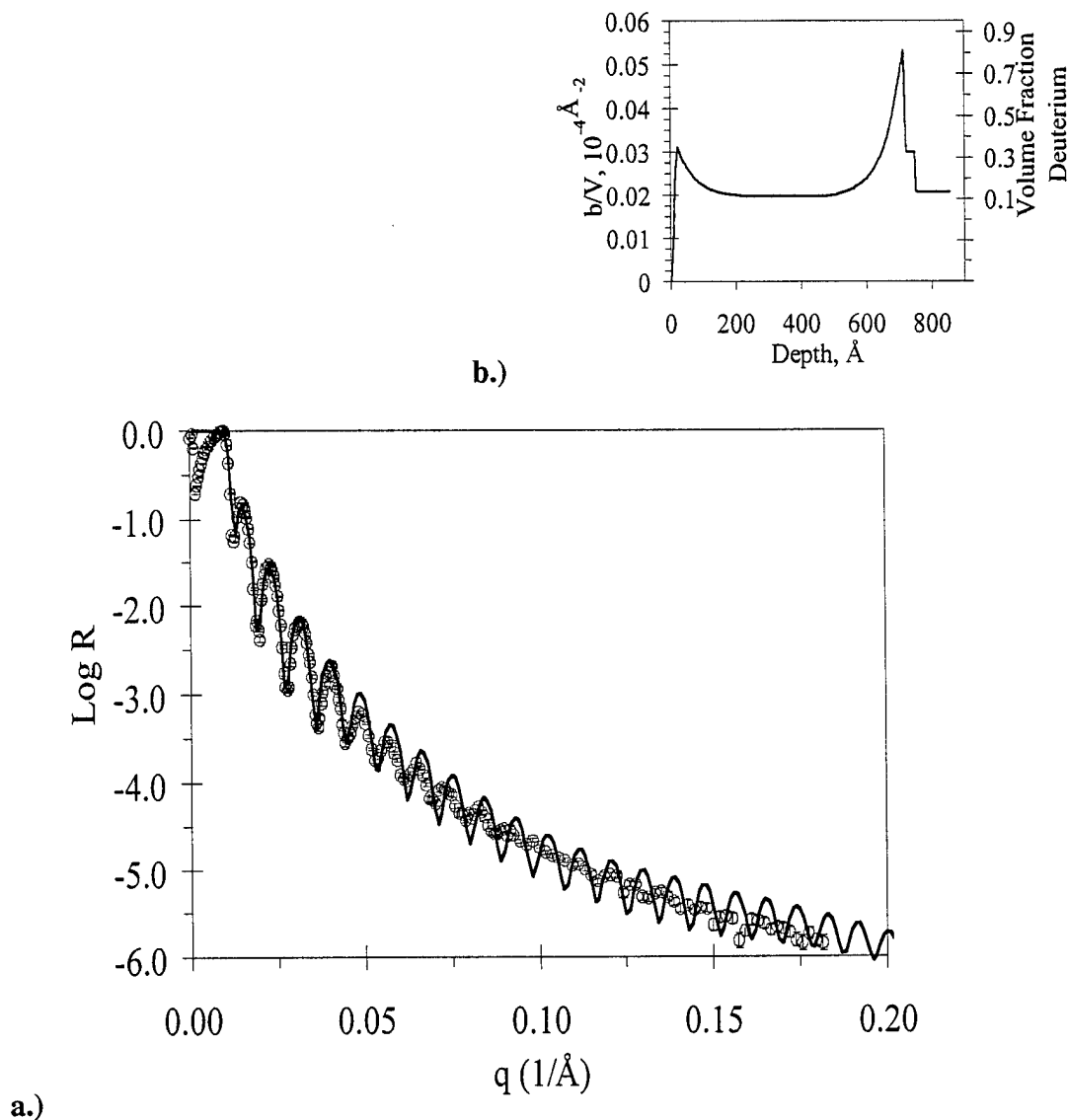


Figure 15. a.) NR corrected data and fit for an annealed blend of 18 wt% 15 arm deuterated DVB linked PS star in hydrogenous linear PS. b.) The corresponding depth profile. Annealing was conducted under high vacuum (10^{-6} Torr) for 7.4 days at 180°C . Upon annealing a higher amount of deuterated star material segregates to the silicon oxide interface.

There is more than one possible explanation for the very similar segregation seen for the h6s and hDVB14s blends. The explanation which suggests itself most readily is that the magnitude of surface segregation is simply not strongly dependent on the number of arms or that an asymptotic behavior is reached as the number of arms increases even over the small range considered here. A

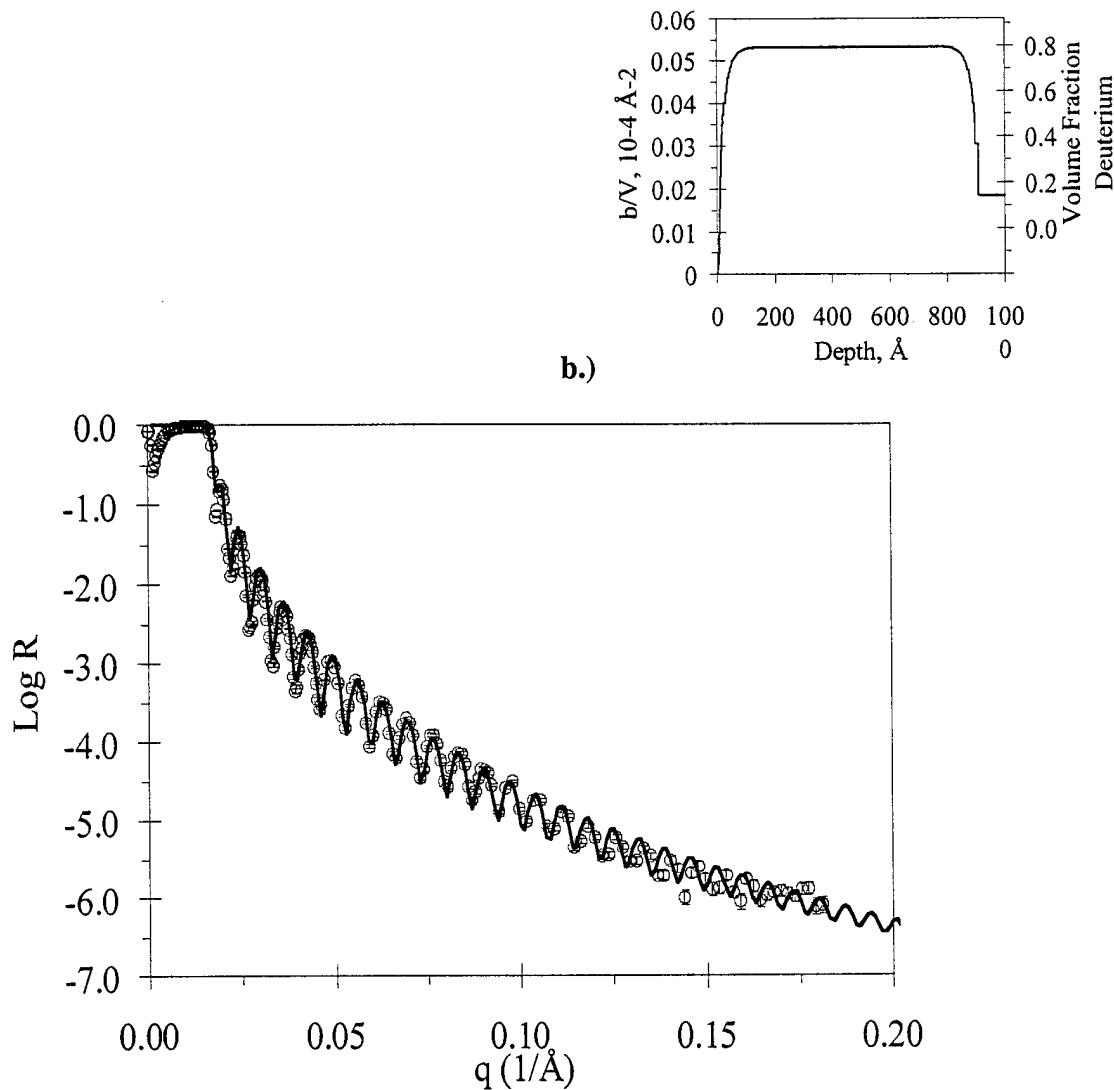


Figure 16. a.) NR corrected data and fit for an annealed blend of 18 wt% 14 arm hydrogenous DVB linked PS star in deuterated linear PS. b.) The corresponding depth profile. Annealing was conducted under high vacuum (10^{-6} Torr) for 7.4 days at 180°C . Upon annealing similar amounts of hydrogenous star material segregate to the air surface and the silicon oxide interface.

second possibility is that the difference in core type is sufficiently important that drawing conclusions about variation with arm number by comparing results from silane-linked stars with those from DVB-linked stars is substantially complicated. The current study does not provide sufficient data to deconvolute the two dependencies. A third possible explanation is that the kinetics of segregation are sufficiently slow that they play an important role here. The molecular weight of hDVB14s is much higher than that of h6s and the difference in functionality will certainly affect the kinetics as well. However, the fact that the segregation to the substrate is so large in the case of the dDVB15s blend is evidence that kinetics are not dominating the results and that the core differences are important. All in all these results are consistent with the contention that variations in segregation with number of arms are modest over the range of numbers probed and that both linking chemistry and segregation kinetics must be investigated further.

Surface Segregation in Polybutadiene Blends

Sample preparation. The preparation of samples containing PB was the same as that for the PS samples except as noted here: PB is a melt at room temperature, meaning that the samples "anneal" to thermal equilibrium under ambient conditions. Unfortunately, the films also tend to dewet with time when stored at ambient conditions. Therefore the samples were "annealed" at room temperature and kept at dry ice temperature otherwise until being measured. For the first measurements reported here there were some difficulties with avoiding water condensation on the samples while warming to room temperature after storage at dry ice temperature. The impact of this water condensation on the sample surfaces, where it occurred, has not been fully assessed.

Results and Discussion. Surface segregation of isotopic blends of linear polybutadiene has not been so extensively studied as that of isotopic blends of linear polystyrene. In fact, the authors are unaware of any published data on isotopically driven surface segregation in linear PB blends. Therefore that effect was measured first by itself. Since the PB is a melt at room temperature, there are challenges in measuring the depth profiles not found in the case of PS. For example, placing the sacrificial layer on the sample for stabilizing the DSIMS etch rate before etching the PB layer is problematic. If PS is used for the sacrificial layer, the etch rate changes when passing from the PS into the PB. The character of this transient is difficult to ascertain. Transferring a layer of PB onto the sample is difficult and if the two PB layers contact one another while in the melt state there will be diffusion across the interface over time. Thus, no DSIMS measurements have been done on the PB samples.

NRA measurements require no sacrificial layer, but the sample should be cooled to minimize beam damage. All NRA measurements made to date on cooled PB samples have shown various artifacts that are still being investigated. Most likely these are due to the condensation of trace water from the vacuum onto the sample surface.

Reflectometry measurements have therefore been key in studying the segregation in absence of either DSIMS or NRA data. Figure 17 presents the NR curve from a blend of 18% linear hPB in 82% linear dPB along with a calculated reflectivity curve from a model believed to properly represent the segregation in the system. The corresponding concentration depth profile of dPB is shown in the inset. The deuterated PB is preferentially segregated to both interfaces as one would expect from the behavior of the polystyrene isotopic blends. The amounts of the deuterated linear PB segregated to the interfaces are summarized in Table 4 along with results for all the PB blends analyzed so far. This surface excess represents the most we would expect to see for the deuterated linear component. As the hydrogenous linear component is replaced with hydrogenous star polymer one would expect at the least a decrease in the amount of deuterated linear PB at the surface. If the architecturally driven segregation were strong enough one would expect the surface to in fact be *depleted* of deuterated linear PB.

The effects of blending linear chains with stars of three different functionalities are seen in Figures 18 and 19. Figure 18 presents the NR curves for the three blends made with 18% star along with model curves fit to the data. Corresponding depth profiles of the concentration of dPB are shown in Figure 19. The fit of the model to the data is outstanding for the sample containing the eight arm star and fair for the other two data sets. The primary difficulty in fitting the data is seen at values of q close to that of the "critical value", q_c , where the reflectivity suddenly drops. An imprecise fit in this region is of primary importance because the segregation manifests itself particularly in this part of the curve. The data from the six arm star blend show a bigger discrepancy between fit and data in this region. Also, for the preliminary analysis shown here the mass balance on deuterated species imposed as a constraint on the concentration profile is not quite met for the six

arm star blend. Therefore the interfacial excesses for that sample may be revised upon further analysis. One clear trend from this data is that the enrichment by deuterated linear PB is always stronger at the air surface than at the substrate interface. The decay lengths of the concentration profiles are of the order expected. *The primary finding from this series of measurements with blends having stars of different functionality is that the architectural effect favoring surface enrichment by the star polymer is much weaker than the isotopic driving force for surface enrichment.* The deuterated linear PB is enriched at the surface in every case. When the number of star arms increases to eight the surface enrichment by deuterated linear PB is decreased, but not by very much. Thus we see here a marked difference from the behavior seen for the polystyrene blends. Clearly it is important to measure blends in which the star is deuterium labeled. Deuterated versions of the four and six arm star have been made and the synthesis of the eight arm PB star is in progress at this writing. Neutron reflectometry beam time for measuring this behavior had been scheduled, but has been delayed due to a prolonged reactor shutdown at NIST.

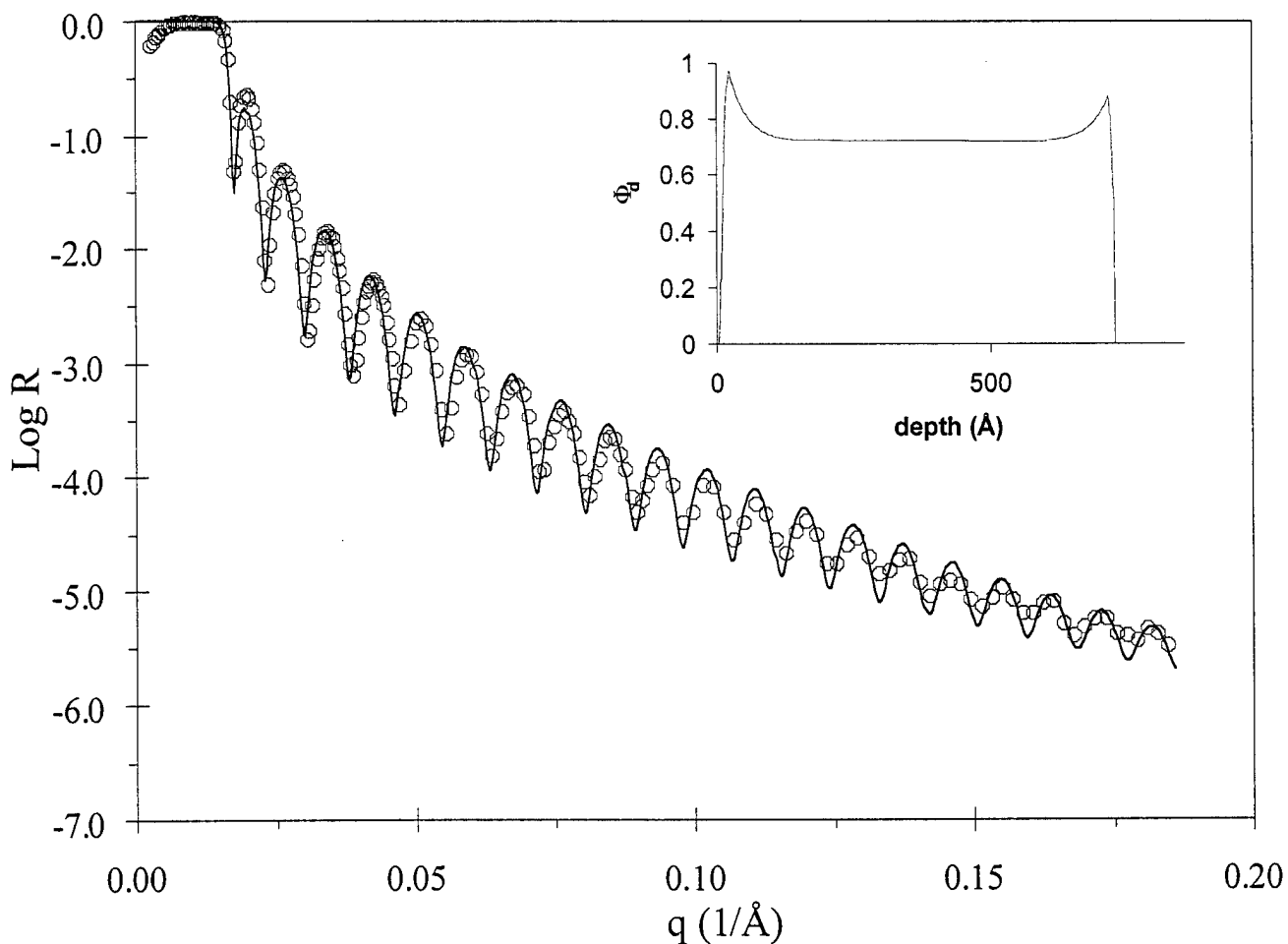


Figure 17. NR corrected data and model fit for blend of 18% linear hPB with 82% linear dPB. The corresponding depth profile of the concentration of deuterated linear PB is shown in the inset.

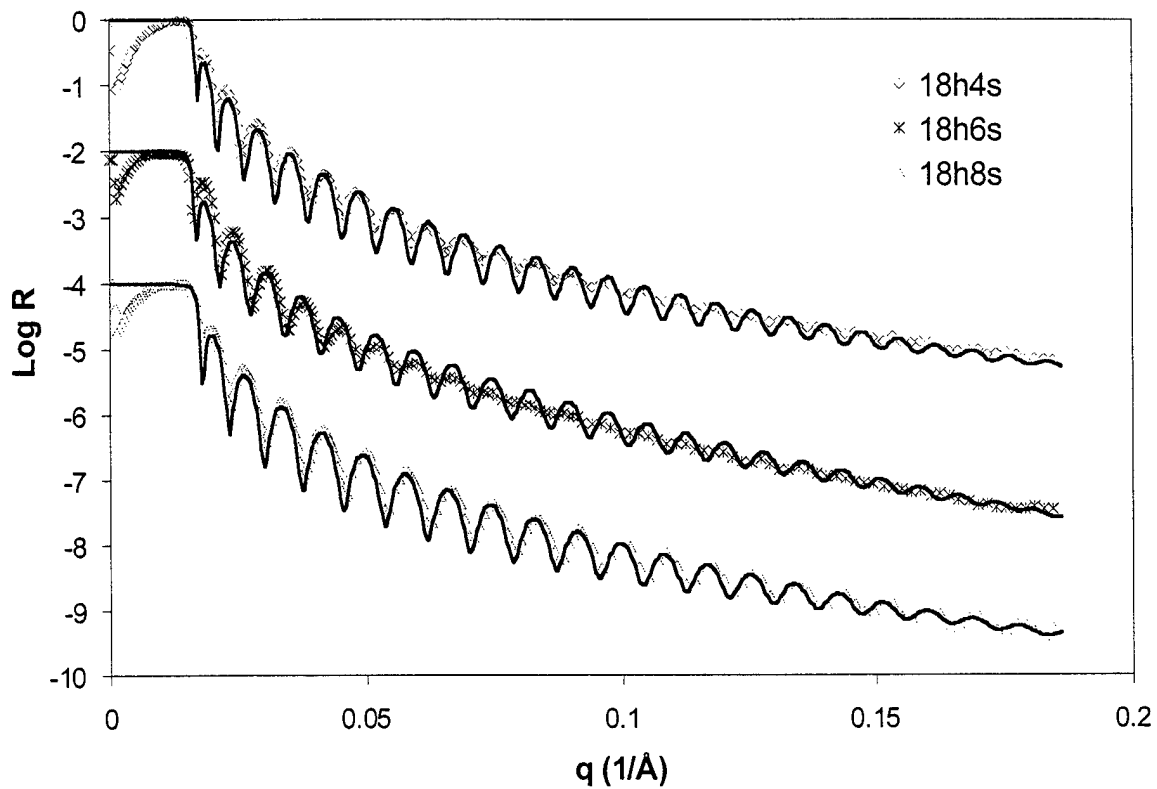
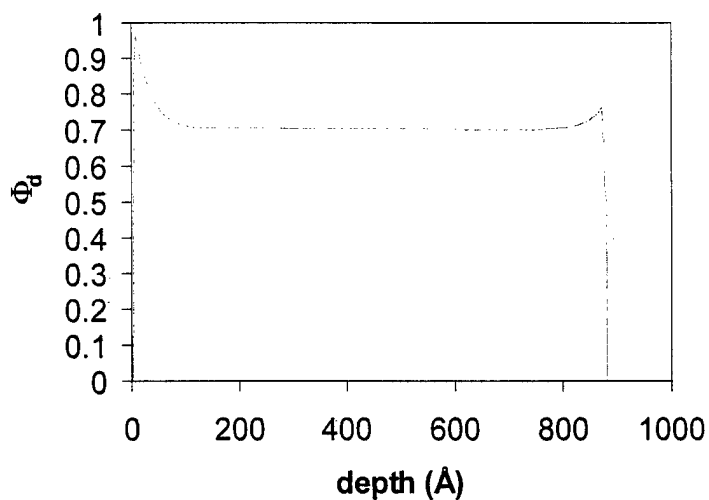
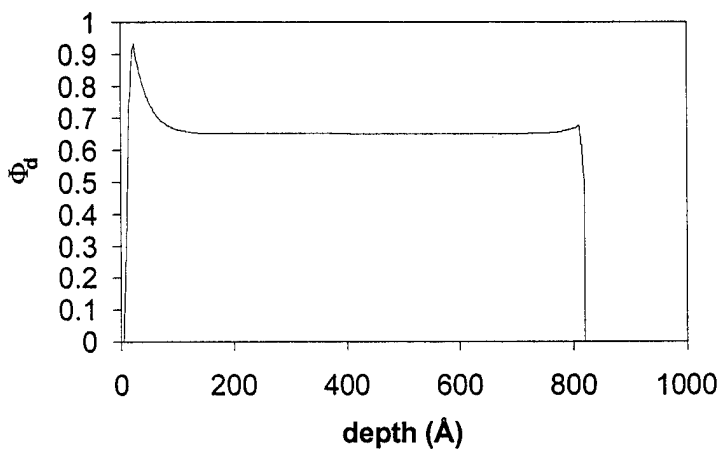


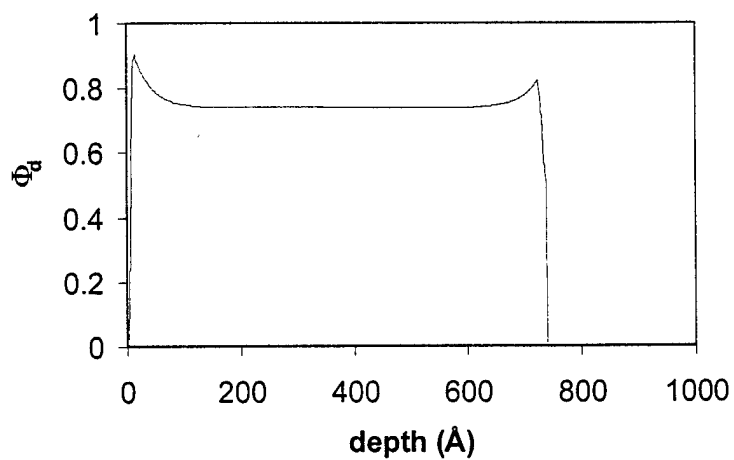
Figure 18. NR curves with best fit model curves for star/linear blends of PB containing 18% star with four arms (top curve), six arms (middle curve), and eight arms (bottom curve).



a.)



b.)



c.)

Figure 19. Depth profiles of the concentration of deuterated linear PB for blends of 18% star and 82% deuterated linear PB with a.) four arm, b.) six arm, and c.) eight arm stars.

Table 4. Surface Excess Values for PB blends

Sample	Annealing Time (days)	Air surface excess (\AA) of dPB	Substrate interface excess (\AA)	SiO _x Present?
hPB/dPB	7.1	8.2	4.8	Yes
18h4s/dPB	7	6.9	1.1	Yes
18h6s/dPB	7.1	7.2	0.1	Yes
18h8s/dPB	7	4.5	2.2	Yes
10h6s/dPB	7	2.5	2.3	Yes
30h6s/dPB	7	6.9	1.6	Yes
18h4s/HMWdPB	7	5.3	1.1	Yes
18h6s/HMWdPB	7	3.9	0.2	Yes

The variation of the surface segregation behavior with concentration of star in the blend was investigated using blends with 10, 30, 50, 70, and 90% six arm star. Reflectivity curves for these blends are shown in Figure 20 and the concentration profiles resulting from analyses of the curves for 10 and 30% are shown in Figure 21. A very good fit has been obtained for the sample with 10% star. The fit for the 30% data is fair and reasonable fits to the remaining data sets have not yet been achieved. The general character of the curves at higher star concentrations suggests that those samples are rougher in some way.

For the sample with 10% star the enrichment with deuterated linear PB is the same at both interfaces and markedly lower than that seen above for the sample with 18% six arm star. In general one may expect that when a minority species enriches the surface the effect is stronger when the minority component is present in smaller concentration. At a concentration of 10% star the surface enrichment due to the opposing effects of architectural differences and isotopic differences are not quite equal, but almost. As one goes to higher concentration of star the isotopic effect dominates. For 30 % star the surface enrichment by deuterated linear PB is nearly three times as large at the surface though it is smaller at the substrate interface. With the results available so far for the concentrations of 10, 18, and 30 it is not possible to identify a clear trend.

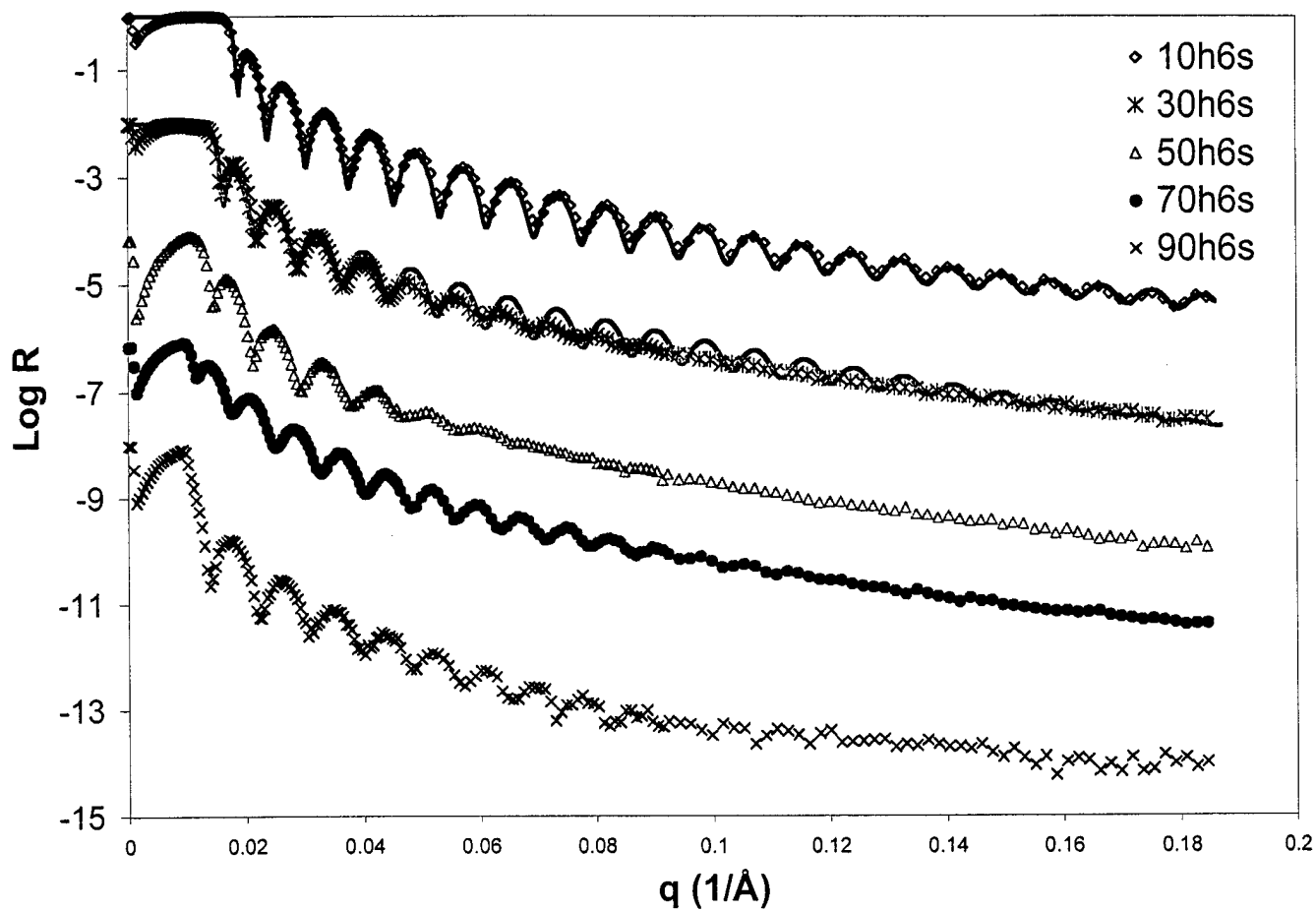
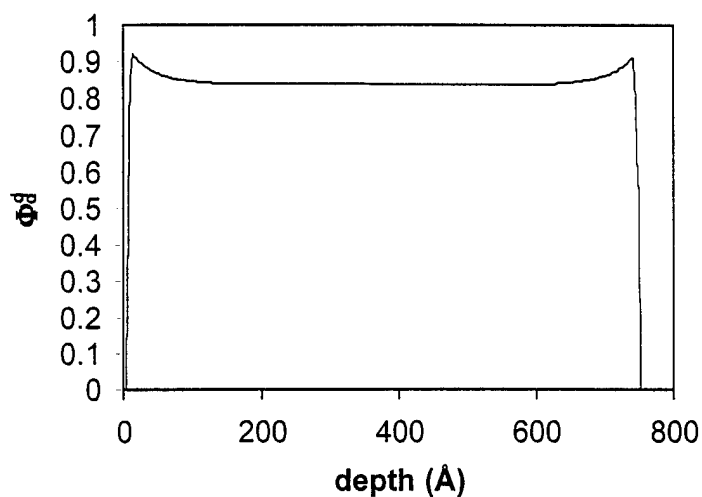
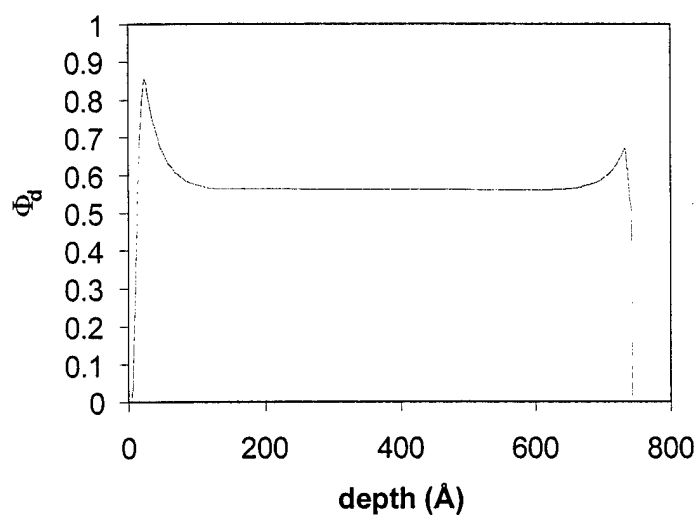


Figure 20. NR curves for blends of six arm star and deuterated linear PB with various concentrations of star. The compositions are, from top to bottom, 10% (open diamonds), 30% (x), 50% (open triangles), 70% (filled circles), 90% (x).



a.)



b.)

Figure 21. Depth profiles of the concentration of deuterated linear PB in blends with six arm star concentrations of a.) 10% and b.) 30%.

NR data for a final type of surface segregation experiment are shown in Figure 22. Here four and six arm star material has been blended with a linear component with a much larger molecular weight, i.e. 364,000 g/mole. In the absence of isotopic effects the segregation of stars to the surface should increase as the molecular weight of the linear component increases. However, for the four arm star the segregation at the surface does not seem to be affected much, while the segregation of deuterated linear chains to the substrate is decreased somewhat, as shown in Figure 23. In the case of the six-arm star, first efforts to fit the data show that again star is depleted from both interfaces, but it remains to optimize the modeling of the data.

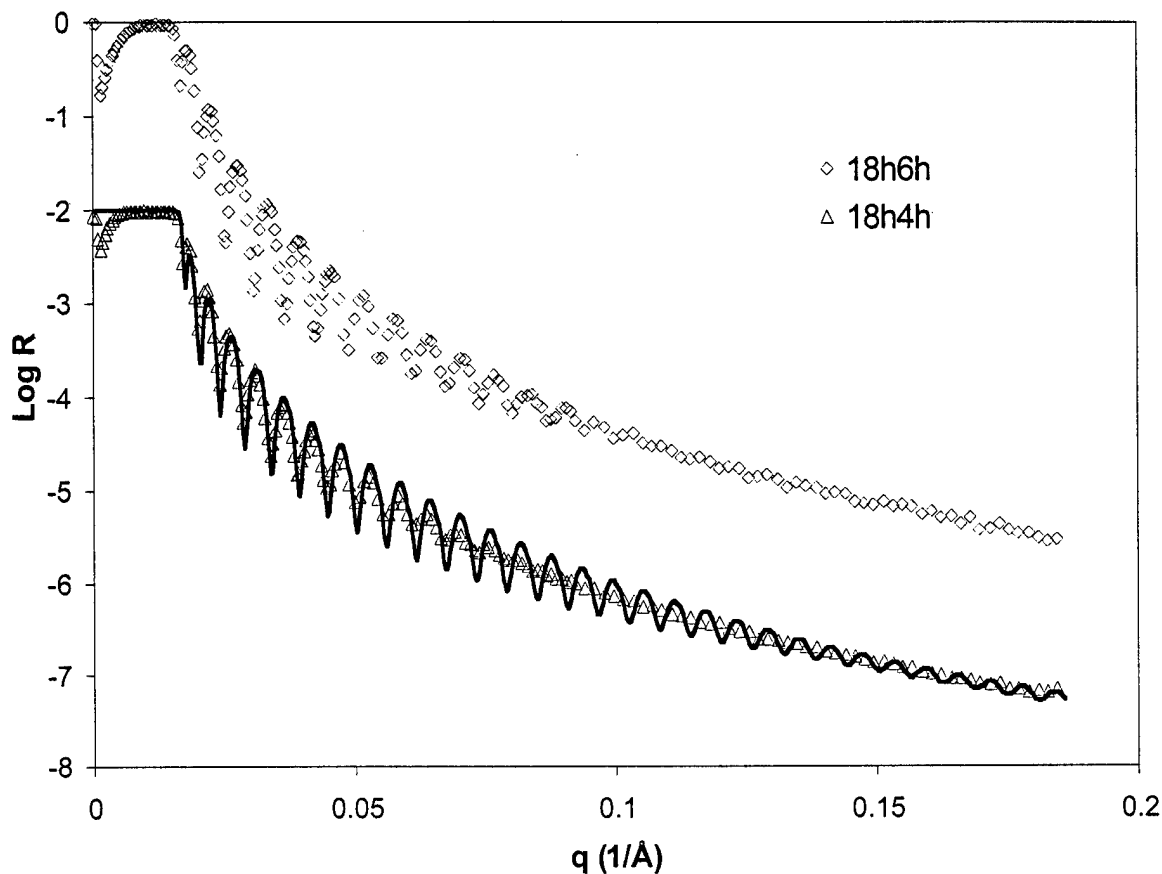


Figure 22. NR curves from blends containing four arm (triangles) and six arm (diamonds) stars with linear chains having a molecular weight (364k) roughly three and a half times those of the stars.

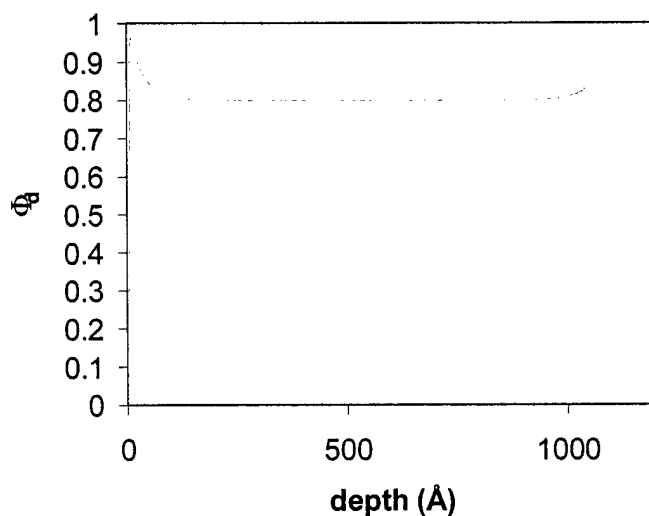


Figure 23. Depth profile of the concentration of high molecular weight deuterated linear PB (364k) in a blend with 18% four arm star.

Conclusions from study of surface segregation

The segregation of regular star-branched chains to both the air and the substrate interfaces of blends with linear analogs has been quantified using three complementary techniques for a small series of well-defined polystyrenes. The segregation to the air interface is seen to increase slightly with small increases in arm number for the chains that are similarly linked. DVB linked stars with many more arms show no greater segregation to the air interface, suggesting that the effect of functionality on degree of segregation is modest. However, the fact that the deuterated DVB-linked star segregates to the silicon oxide surface four times as strongly as does the silane-linked star with roughly half as many arms suggests that differences in core chemistry play a non-negligible role.

In the case of polystyrene the architectural effect prevails over the isotopic effect in determining the species preferred at the surface. Indeed, the hydrogenous stars go more strongly to the air surface than do deuterated stars, quite in contrast to expectations that the isotopic effect and architectural effect would reinforce one another to give the strongest surface segregation for the deuterated stars. At the substrate interface the enhancement of segregation of the deuterated species when the oxide is present is seen for stars just as it has been seen for linear chains²⁰. Deconvolution of the contributions of the core type, chain ends, and branching to segregation will necessitate further measurements with carefully designed molecules.

The picture of the behavior of blends of polybutadiene is much less complete, but a few conclusions can be drawn. For small numbers of arms, the stronger isotopic effect for PB dominates the architectural effect so that in blends labeled for measurements the linear species may be preferentially located at the surface. We anticipate that in the absence of labeling the star will go to both the surface and substrate interface, but not so strongly as in the case of polystyrene. The strength of the segregation is not much changed by a nearly four-fold change in the molecular weight of the linear component.

IV. DYNAMICS: COMPARISON OF STAR AND LINEAR POLYBUTADIENE

Dynamics in blends of star and linear materials are also of interest, even though they are not the focus of this effort. In 1999 the PI had the opportunity to collaborate with Prof. Alexei Sokolov of the University of Akron and Dr. Brian Annis of Oak Ridge National Laboratory to make neutron inelastic scattering measurements of the dynamics of the star-branched butadiene. Before considering the effects found in blends it was important to consider first the pure star materials. *The specific objective of these measurements was to probe the collective dynamics of star polybutadiene polymers (PB) to see how these dynamics differ from those of linear analogs both below and above the glass transition.*

It is to be anticipated that the collective dynamics will be affected by chain architecture as well, at least under some conditions. The dynamics of regular star branched polymers in the melt have already been studied some theoretically²², experimentally^{23,24}, and by simulation²⁵. The focus of nearly all of the theoretical, experimental and simulation work has been on the dynamics of translational diffusion and rheology, where the behavior of the arms has been of particular interest. A notable exception has been an experimental study of Bershtein *et al.*²⁶ which considered changes in the glass transition behavior of polymers when attached to fullerenes to form stars. In that work the authors contended, on the basis of differential scanning calorimetry experiments, that the cooperativity of the motions was disrupted by the tethering of chains to a core. The focus of our

measurements was the collective dynamics at low energy (< 10 meV), e.g. the so-called boson peak and the fast picosecond relaxation. To our knowledge such measurements had not been studied experimentally by others for any star system, nor had there been any theoretical work published on this topic.

It is thought that these collective dynamics involve cooperative motion of segments from several chains²⁷ in regions of order 10-20Å in size. The key question of the work was how do these collective dynamics change when the chains are confined by the tethering to a star core? Will the cooperativity in the motion break down? It was opportune to study the low vinyl content PB stars because the dynamics of PB linear chains have already been studied very extensively, not only with inelastic neutron scattering, but also with Raman spectroscopy^{27,28} and rheological methods²⁹.

Two of the well-defined, hydrogenous polybutadiene star polymers synthesized by Prof. Quirk's group were studied. The first was the four arm star with arm molecular weight of 24k and the other the six arm star with arm molecular weight of 18.7k. Thus the overall molecular weights were 96k and 112k. A linear analog with molecular weight similar to that of the whole star (88k) was studied as well as a basis for comparison.

The inelastic scattering was measured using the spectrometer "QENS" at Argonne National Laboratory over a q range of 0.5-2.5 Å⁻¹. Vanadium data was used to correct the detector response. One measurement was made at 5 K to quantify the background and instrumental broadening. For each star, measurements were taken at various temperatures over the range of temperature from 100 K to about room temperature, which is considerably above T_g (ca. 180K). This allowed us to look for changes due to tethering on both sides of the glass transition. For the linear analog it was only necessary to measure at two temperatures (lowest and highest), as a body of data is available in the literature as well. The data were analyzed using the traditional incoherent approximation, taking into account multiple scattering.

The data are plotted in Figure 24 in the form of structure factors as a function of scattering vector, q . No differences in the dynamics of the linear and star-branched chains are seen for either the four-arm or six-arm stars. In addition the linear and star chain dynamics are the same above and below the glass transition. The results indicate that for arms of these lengths (several times the entanglement molecular weight) the tethering to the core plays no role in the low energy collective dynamics. In future work it will be of interest to consider the case in which the arms are much shorter.

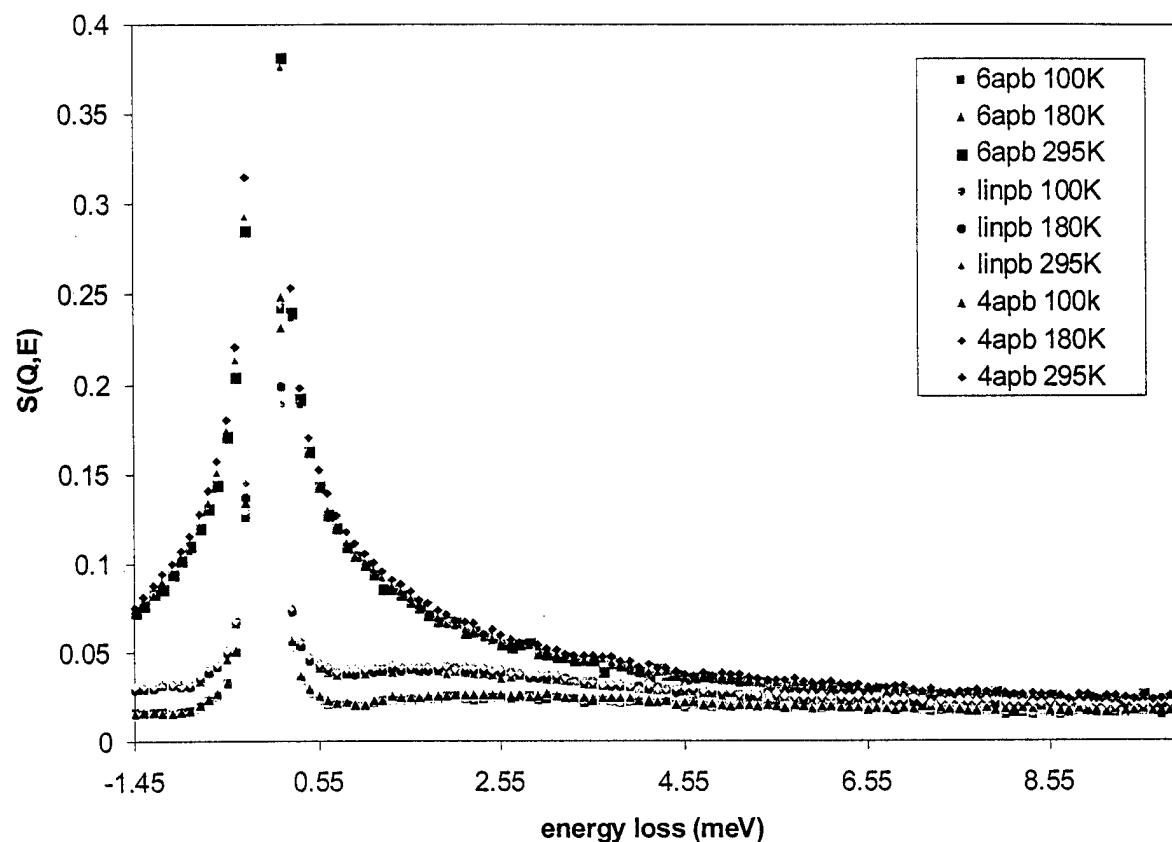


Figure 24. Dynamical structure factor for PB chains of three types, linear, four arm star, and six arm star, measured at three temperatures as indicated in the legend. The three types of chains behave essentially identically at each temperature.

REFERENCES

- (1) Hawker, C. J. *J. Am. Chem. Soc.* **1994**, *116*, 11314.
- (2) Mays, J. W.; Hadjichristidis, N.; Fetters, L. J. *Macromolecules* **1985**, *18*, 2231.
- (3) Zimm, B. H.; Stockmayer, W. H. *J. Chem. Phys.* **1949**, *17*, 1301.
- (4) Glinka, C.; Barker, J.; Hammouda, B.; Krueger, S.; Moyer, J.; Orts, W. *J. Appl. Cryst.* **1998**, *31*, 430.
- (5) Bates, F. S.; Wignall, G. D. *Phys. Rev. Lett.* **1986**, *57*, 1429.
- (6) Greenberg, C. C.; Foster, M. D.; Turner, C. M.; Corona-Galvan, S.; Cloutet, E.; Butler, P. D.; Hammouda, B.; Quirk, R. P. *Polymer* **1999**, *40*, 4713.
- (7) deGennes, P. G. *Scaling Concepts in Polymer Physics* Cornell University Press, Ithaca, NY, **1979**.

- (8) Hammouda, B. *Adv. Polym. Sci.* **1993**, *106*, 87.
- (9) Fredrickson, G.H.; Liu, A.; Bates, F. S. *Macromolecules* **1994**, *27*, 2503.
- (10) Londono, J. D.; Narten, A. H.; Wignall, G. D.; Honnell, K. G.; Hsieh, E. T.; Johnson, T. W.; Bates, F. S. *Macromolecules* **1994**, *27*, 2864.
- (11) Graessley, W. W.; Krishnamoorti, R.; Balsara, N. P.; Fetters, L. J.; Lohse, D. J.; Schultz, D. N.; Sissano, J. A. *Macromolecules* **1993**, *26*, 1137.
- (12) Rhee, J.; Crist, B. C. *Macromolecules* **1993**, *28*, 4174.
- (13) Balsara, N. P.; Lose, D. L.; Graessley, W. W.; R., K. *J. Chem. Phys.* **1994**, *100*, 3905.
- (14) Bates, F.S.; Dieker, S.B.; Wignall, G.D., *Macromolecules*, **1986**, *19*, 1938.
- (15) Foster, M. D. *Critical Reviews in Analytical Chemistry* **1993**, *24*, 179.
- (16) Klein, J. *Science* **1990**, *250*, 640.
- (17) Giesler, K.-H.; Endish, D.; Rauch, F.; Stamm, M. *Fresenius J. Anal. Chem.* **1992**, *346*, 151.
- (18) Tesmer, J. R.; Nastasi, M.; Barbour, J. C.; Maggiore, C. J.; Mayer, J. W. *Handbook of Modern Ion Beam Materials Analysis*, Materials Research Society, Pittsburgh, PA, 1995.
- (19) The surface excess is defined by an integral representing the area between two concentration profiles, one corresponding to the case of a film of composition which does not change with depth and a second corresponding to the case in which the composition at the surface (interface) is enriched. When the composition is expressed in volume fraction and depth is given in Angstroms this area has units of Angstroms.
- (20) Hariharan, A.; Kumar, S. K.; Rafailovich, M. H.; Sokolov, J.; Zheng, X.; Duong, D.; Schwarz, S. A.; Russell, T. P. *J. Chem. Phys.* **1993**, *99*, 656. (21) Wu, D. T.; Fredrickson, G. H. *Macromolecules* **1996**, *29*, 7919.
- (21) Wu, D. T.; Fredrickson, G. H. *Macromolecules* **1996**, *29*, 7919.
- (22) Blottiere, B.; McLeish, T. C. B.; Hakiki, A.; Young, R. N.; Milner, S. T. *Macromolecules* **1998**, *31*, 9295.
- (23) Semenov, A.N.; Vlassopoulos, D.; Fytas, G.; Vlachos, G.; Fleischer, G.; Roovers, J. *Langmuir* **1999**, *15*, 358.
- (24) Pakula T., Vlassopoulos, D.; Fytas, G.; Roovers, J. *Macromolecules* **1998**, *31*, 8931.
- (25) Sikorski, A.; Romiszowski, P. *J. Chem. Phys.* **1996**, *104*, 8703. Sikorski, A.; Kolinski, A.; Skolnick, J., *Macromol. Theory Simul.* **1994**, *3*, 715. Pakula, T. *Comp. Theor. Polym. Sci. S 8: (1-2) Part 2 Sp. Iss. SI.* **1998**, *21*.
- (26) Bershtein, V. A.; Egorov, V. M.; Egorova, L. M.; Sysel, P.; Zgonnik, V. N. *J. Non-Cryst. Solids* **1998**, *235-237*, 476.
- (27) Buchenau, U. Pecharroman, C.; Zorn, R.; Frick, B. *Phys. Rev. Lett.* **1996**, *77*, 4035.
- (28) Sokolov, A.P.; Novikov, V.N.; Strube, B. *Phys. Rev. B* **1997**, *56*, 5042.
- (29) Zorn, R.; McKenna, G.B.; Willner, L.; Richter, D. *Macromolecules* **1995**, *28*, 8552.

TECHNOLOGY TRANSFER

The text in this section is arranged as requested by the program monitor.

a.) Exchange of samples and collaborations with the Army and industry

Two collaborations with Army scientists have been in progress in the last year. Nuclear reaction analysis measurements were carried out in the ion beam analysis laboratory at the ARL Rodman Laboratory with Drs. Jim Hirvonen and Derek Demaree. Members of the UA team were there at least three times to make measurements or discuss the work. Additional measurements were made by Dr. Demaree on samples that had been left at ARL.

Samples were also sent to Dr. Mark Woodward, then at the Shady Grove site (now at Aldephi) to run secondary ion mass spectroscopy measurements. Time-of-flight static SIMS measurements were arranged by Dr. Woodward with a collaborator at the National Institute of Standards and Technology. Dr. Woodward assisted in the subsequent analysis of the data.

b.) Patent Applications and/or awards

There were no patent applications.

c.) Names and organization of individuals in government, academy, or industry to whom last year's report was sent and/or this year's report will be sent:

Paul Butler and Boualem Hammouda, NIST
Dr. Wen-li Wu, Dr. Barry Bauer, NIST
Dr. Wendel Shuely, ERDEC
Dr. Nora Beck Tan, ARL
Dr. Robert Reeber, ARO
Dr. Bill Mullins, ARO
Dr. Derek Demaree, ARL
Dr. Jim Hirvonen, ARL

Priv. Doz. Henning Menzel, University of Hannover
Prof. Puru Gujrati, The University of Akron
Prof. G. Strobl, University of Freiburg
Dr. Matt Muir, Dr. David Trowbridge, Dr. Michael Ambler, Dr. John Willey
The Goodyear Tire & Rubber Company
Dr. Georg Böhm, Manager, Bridgestone/Firestone Research, Akron
Prof. Jeffrey Koberstein, Formerly of U. Conn., now Columbia U.

d.) Face-to-face Interactions with Army, DoD, Industry or Academic personnel

In previous years of the award period the work was discussed with the following individuals. Individuals who have assisted with this work in some way as collaborators are marked as such.

Craig Hawker, IBM Almaden - collaborator
Jack Price, U.S. Naval Lab (White Oaks)- collaborator
Paul Butler and Boualem Hammouda, NIST - collaborators

Prof. Tobin Marks, Northwestern University
Priv. Doz. Henning Menzel, University of Hannover
Dr. Barry Bauer, NIST
Dr. Nora Beck Tan, ARL
Prof. Frank S. Bates, University of Minnesota
Prof. Puru Gujrati, The University of Akron
Prof. Erhard Fischer, Priv. Doz. Thomas Vilgis, Priv. Doz. Jürgen Rühle, Priv. Doz. Tadeus Pakula,
Priv. Doz. Manfred Stamm, Max-Planck-Institut für Polymerforschung.
Prof. G. Strobl, University of Freiburg
Dr. Matt Muir, Dr. David Trowbridge, Dr. Michael Ambler, Dr. John Willey
The Goodyear Tire & Rubber Company - some assistance with light scattering from DT
Dr. Georg Böhm, Manager, Bridgestone/Firestone Research, Akron
Dr. Wendel Shuely, ERDEC
Dr. Jürgen Rühle, Max-Planck-Institut für Polymerforschung
Dr. Manfred Stamm, Max-Planck-Institut für Polymerforschung

This year the work has been discussed in addition with the following persons:

Dr. Derek Demaree, ARL - collaborator
Dr. Jim Hirvonen, ARL - collaborator
Dr. Mark Woodward, ARL - collaborator
Prof. David Haddleton, University of Warwick - collaborator
Prof. Alexei Sokolov, University of Akron - collaborator
Dr. Brian Annis, Oak Ridge National Laboratory - collaborator
Dr. Steve McKnight, ARL
Prof. Edward (Ned) Thomas, M.I.T.
Dr. Scott Milner, Exxon Research & Engineering Company
Dr. Andreas Heise, DSM, Netherlands
Dr. Bob Miller, IBM Laboratory, Almaden, California
Prof. Schuster, Deutsche Institut für Kautschuktechnologie
Prof. Ken Shull, Northwestern University
Dr. Ken Schweitzer, U. Illinois
Prof. Arun Yethiraj, U. Wisconsin
Prof. Anne Mayes, MIT
Prof. Tom Russell, U. Mass. Amherst
Drs. C. Fleischer and J. Elman from Kodak
Prof. J. Mays, U. Alabama

e.) Breakthroughs

Experimental determination of the thermodynamic interaction between regular long-branched molecules and their linear counterparts had never been done before. This will impact individuals in industry who are designing products and processes involving blends of long-branched and linear chains. Specifically, practitioners now have experimental confirmation of the following general guideline from theory:

- Mixing stars and linear chains should give single phase systems unless the molecular weights are very high

- In contrast, mixing comb and linear polymers can readily lead to phase separation at moderate molecular weights.

f.) Interactions with other ARO PIs.

The work has been discussed at various points with Prof. Jeff Koberstein.

g.) Students working for or traveling to Army or DoD installations

Three students, Teresa Zook Martter, Carmen Greenberg, and Jongwhi Hwang, have done measurements with Army personnel in the ion beam laboratory at the ARL Rodman laboratory and/or the ion beam laboratory at the White Oaks lab (the only naval laboratory still located there at the time). Two other students, Tricia Cregger and Zhihao Chen, have also observed some of the ion beam measurements at the White Oaks laboratory, although they were not directly involved in the measurements.

A former student on this project, David Teale took a position with the Army in the last year. He is in the night vision laboratory at Ft. Belvoir, Virginia.

h.) Leveraging of Army funds

This project has attracted interest from two laboratories interested in providing polymer samples for the study of blends of branched and linear chains. The comb branched molecule discussed above was made by Dr. Craig Hawker at the IBM Almaden laboratory. Dr. Hawker also provided another comb polymer and other measurements will be done with these materials in the future.

At the 1999 American Physical Society Meeting in March 1999 Bob Miller, also from the IBM Almaden laboratory, planned with Prof. Foster for the study of blends containing stars made with dendrimer cores. Some materials were made, but the definition of the functionality of the first samples proved to be insufficient for incisive measurements and the postdoctoral associate working on that project moved to a permanent position in industry in Europe. That collaboration is currently on hold.

Prof. David Haddleton from the University of Warwick visited Akron and was intrigued by our ability to study interactions between chains of different architecture. He is currently making several samples of long-branched poly(methylmethacrylate) which will be used to study the issues raised here further. Beamtime at NIST has already been awarded to the Prof. Foster for these measurements.

FMC, Lithium Division provided the *sec*-BuLi initiator used for the synthesis. Goodyear donated deuterated butadiene for the synthesis of deuterated polybutadiene.